TELLURIUM-INDUCED CORROSION OF STRUCTURAL ALLOYS FOR
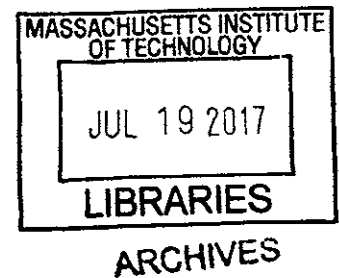NUCLEAR APPLICATIONS IN MOLTEN SALTS

by

Natasha Skowronski

SUBMITTED TO THE DEPARTMENT OF NUCLEAR SCIENCE AND
ENGINEERING IN PARTIAL FULFILLMENT OF THE REQUIREMENTS
FOR THE DEGREE OF BACHELOR OF SCIENCE IN NUCLEAR
SCIENCE AND ENGINEERING AT THE MASSACHUSETTS INSTITUTE
OF TECHNOLOGY

JUNE 2017

Signature of Author: _Signature redacted_

Natasha Skowronski
Department of Nuclear Science and Engineering
May 26, 2017

Signature redacted

Certified by:_____

Michael Short
Assistant Professor of Nuclear Science and Engineering
Thesis Supervisor

Signature redacted

Accepted by:_____

Michael Short
Assistant Professor of Nuclear Science and Engineering
Chairman, NSE Committee for Undergraduate Students

TELLURIUM-INDUCED CORROSION OF STRUCTURAL ALLOYS FOR NUCLEAR APPLICATIONS IN MOLTEN SALTS

by

Natasha Skowronski

Submitted to the Department of Nuclear Science and Engineering on May 26, 2017 in partial fulfillment of the requirements for the degree of Bachelor of Science in Nuclear Science and Engineering.

ABSTRACT

The mechanism by which tellurium causes intergranular corrosion (IGC) of structural alloys in molten salt reactors is currently poorly understood. Limited corrosion testing has been performed on a few select alloys in simulated reactor conditions. In this thesis, the results of performing 50 h, 100 h, and 150 h corrosion tests on alloys Hastelloy N, Nickel-201, Incoloy 800H, and 316L Stainless Steel are presented. Upon inspection of the corroded surfaces of each alloy after its immersion in molten LiF–NaF–KF (FLiNaK) salt at 700 °C using scanning electron microscopy (SEM) and energy-dispersive x-ray spectroscopy (EDS), a consistent corrosion rate could not be determined for any of the alloys, nor could confident identification of telluride compounds within the corrosion layer or grain boundaries of any alloy be made. However, the results did appear to confirm the importance of using a low oxygen environment and avoidance of galvanic corrosion during testing. Furthermore, preliminary results from EDS analysis of one alloy sample implied that, with improved count rates taken during the elemental identification process, tellurium may be more clearly revealed in the corrosion layers and grain boundaries of the alloys tested.

TELLURIUM-INDUCED CORROSION OF STRUCTURAL ALLOYS FOR NUCLEAR APPLICATIONS IN MOLTEN SALTS

NATASHA SKOWRONSKI

CONTENTS

LIST OF FIGURES

LIST OF TABLES

ACKNOWLEDGEMENTS

ABSTRACT

The mechanism by which tellurium causes intergranular corrosion (IGC) of structural alloys in molten salt reactors is currently poorly understood. Limited corrosion testing has been performed on a few select alloys in simulated reactor conditions. In this thesis, the results of performing 50 h, 100 h, and 150 h corrosion tests on alloys Hastelloy N, Nickel-201, Incoloy 800H, and 316L Stainless Steel are presented. Upon inspection of the corroded surfaces of each alloy after its immersion in molten LiF-NaF-KF (FLiNaK) salt at 700 °C using scanning electron microscopy (SEM) and energy-dispersive x-ray spectroscopy (EDS), a consistent corrosion rate could not be determined for any of the alloys, nor could confident identification of telluride compounds within the corrosion layer or grain boundaries of any alloy be made. However, the results did appear to confirm the importance of using a low oxygen environment and avoidance of galvanic corrosion during testing. Furthermore, preliminary results from EDS analysis of one alloy sample implied that, with improved count rates taken during the elemental identification process, tellurium may be more clearly revealed in the corrosion layers and grain boundaries of the alloys tested.

1 INTRODUCTION

1.1 The Need for a Waste–Annihilating Reactor

The only design amongst the fourth generation of nuclear reactor designs to use fuel dissolved into its coolant, the Molten Salt Reactor (MSR) has potential to make profound impact on the world. The MSR, due to its unique fuel-coolant mixture, has the capacity to consume spent nuclear waste and convert it into energy. It is also expected to have passive safety systems that allow for designs to be walk-away safe, as well as dramatically increased efficiency in fuel-to-power conversion relative to today's current solid-fuel reactors. This combination of features amounts to a powerful tool in the face of a society in need of both energy and a solution for nuclear waste.

However, a new reactor design begets new design challenges. Many of the challenges faced by the MSR design are related to its materials, given the molten salt environment that it must safely contain. The idea behind the MSR design is that molten salt coolant has the thermal properties to remove decay heat effectively from the nuclear reaction during reactor operation, while at the same time requiring no pressure to remain in a liquid form. This property is a key difference relative to, say, a pressurized water reactor (PWR) where liquid water coolant can flash to steam and lose its ability to keep the reactor at a safe temperature if pressure in the system is somehow lost due to accident. The salts proposed for MSR designs, often including lithium-fluoride, typically melt at temperatures above $700\,^{\circ}C$, so materials capable of withstanding both high temperatures and any corrosive properties of the molten salts are required.

One class of materials challenges anticipated in designing an MSR is that of corrosion due to fission products contained inside the fuel-salt mixture. These fission products, including a wide variety of elements, can form compounds with the compositional elements in a given alloy and attack it at its grain boundaries. In particular, the fission product tellurium has been found to cause intergranular corrosion (IGC) of nickel-based superalloys in molten salt environments [1, 2, 3, 4]. Because nickel-based superalloys have been proposed as potential structural alloys for containing the fuel-salt mixture of an MSR, the stress that such a structure would need to withstand could also contribute to stress corrosion cracking (SCC), a form of corrosion that results when an alloy suffers the combination of a corrosive environment and mechanical stress.

1.2 The Need for Materials Testing

To address the issue of tellurium-induced intergranular corrosion, data must be collected on the severity and extent to which tellurium corrodes particular alloys in a molten salt environment. Analyzing images taken of different alloys that have been exposed to fission-product-containing molten salts for many hours will help to reveal which of those alloys most resists corrosion and which mechanisms are contributing to corrosion. It is here proposed that, upon analysis of alloy samples subjected to corrosion testing in the molten salt FLiNaK, consisting of lithium fluoride (LiF), sodium fluoride (NaF) and potassium fluoride (KF), mixed with the fission product tellurium (Te) in nickel(II) telluride form will induce relatively increased corrosion into samples of Hastelloy N, Incoloy 800H, Nickel 201, and 316L Stainless Steel through a coupled mechanism of diffusing into the grain

boundaries of the alloy and simultaneous attraction and formation of each alloy's compositional elements into intermetallic compounds.

2 BACKGROUND

2.1 Historical Overview of Alloy Corrosion in Molten Salts

The concept for the MSR has its origins in the Aircraft Reactor Experiment (ARE) and the Molten Salt Reactor Experiment (MSRE), experiments conducted at Oak Ridge National Laboratory (ORNL) between the 1940s and the 1970s which pioneered the use of dissolved nuclear fuel in molten salt coolant [5]. Based on the high fuel salt operation temperature needs for a molten salt breeder type reactor envisioned for powering aircraft, the ARE originally used Inconel 600, a nickel-chromium-based superalloy.

However, once it had been determined that Inconel 600 had insufficient strength and corrosion characteristics, exploration began into the Hastelloy family of nickel-based superalloys, starting with Hastelloy B (Ni–28% Mo–5% Fe) and Hastelloy W (Ni–25% Mo–5% Cr–5% Fe) [6]. Again, after various problems arose with these alloys, including rapid embrittlement, age-hardening, poor fabrication ability, and oxidation resistance, new testing demonstrated that nickel-based alloys would have fewer of these issues than the iron-based alloys being tried. Thus was a new alloy designed specifically for the environment of the molten salts used in the ORNL experiments called Hastelloy N (Ni–16% Mo–7% Cr–5% Fe–0.05% C) [6].

Hastelloy N shows excellent corrosion resistance to molten fluoride salts, is structurally stable at the high operating temperatures demanded by an MSR, is easily fabricated into the complex pieces needed for nuclear reactor components, and is weldable [6]. However, after initial tests run with the MSRE using Hastelloy N as a structural material, it was found that it showed susceptibility to stress corrosion cracking (SCC) [7]. These cracks were determined as early as 1975 to be the result of intergranular corrosion due to tellurium, a fission product generated in the fuel-salt mixture during operation [7].

2.2 Stress Corrosion Cracking

Stress corrosion cracking occurs when a tensile stress on a material in a corrosive environment results in cracking in the material earlier than it otherwise would have occurred [8]. Although SCC can be made possible with intergranular corrosion, SCC itself only happens in the presence of stress, distinguishing it from localized IGC. Attention must be given to SCC when developing the structural materials of an MSR because of the potential it has to shorten the lifespan of the structure. As seen in Figure 1, the corrosive environment from which SCC stems ultimately leads to a shorter strain to failure and a reduced maximum stress, thus compromising the integrity of the material during operation. Such compromised materials not only could severely hinder the economic potential of any commercial MSR if it cannot operate as long as needed to see return on investment, but also might result in catastrophic accidents if not addressed. Based on the MSRE conducted at ORNL, the diffusion depth of Te into alloy was found to be approximately 125 µm–325 µm after 30 years of operation [1].
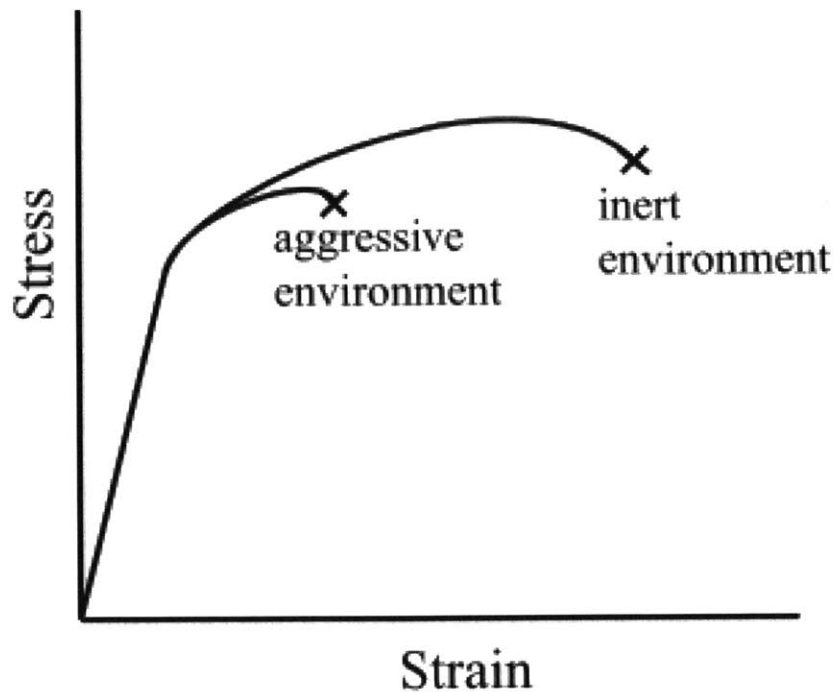
Figure 1: Effect of the environment on stress-strain behavior of metals undergoing stress corrosion cracking [8].

2.3 Literature Review

Recent research has investigated from first principles the methods by which Te enters the grain boundary (GB) of nickel in an attempt to explain some of the mechanisms at work in the SCC of Hastelloy N in the corrosive environment of molten salts. Tellurium preferentially occupies substitutional sites of lowest binding energy at the GBs, thus inducing GB expansion due to Te's relatively larger atomic size when compared with that of Ni [9]. Therefore, though grains in alloys are known to be responsible for great structural advantage when it comes to slowing dislocation movement and increasing strength and ductility, they are also sites for potential weakening and embrittlement if care is not taken to mitigate corrosion processes in the environments intended for the material.

Prior to the early 2000s, research into mitigating the effects of IGC by Te on Hastelloy N explored primarily alloy compositions and electrochemical strategies. The strategies proposed between approximately 1970 and 2000 include doping Hastelloy N with 2 % Nb, increasing the amount of Ti in the composition, adding Cr to the composition, creating homogenized titanium-modified Hastelloy N, and reducing the oxidation potential of the fuel salt to below 70 [7, 10, 11, 12]. As shown in Figures 2 and 3, Nb concentration, as well as fuel salt oxidation potential, were found to have an important correlation with crack frequency and depth. These experiments, many of which concluded with reduction or lack of IGC due to Te, have served as an important starting place for more recent studies, which further explore and confirm some of the older results focusing on alloy composition and fuel salt reduction potential while also investigating some theoretical mechanisms involved in the corrosive process.

Figure 2: Variations of severity of cracking with Nb content. Samples were exposed for the indicated times to salt-containing Cr_3Te_4 and Cr_5Te_6 at 700 °C. Reproduced from Mc Coy, H. E.; *et al.* Status of materials development for molten-salt reactors, ORNL-TM-5920; ORNL: Oak Ridge, TN, 1978 [6].
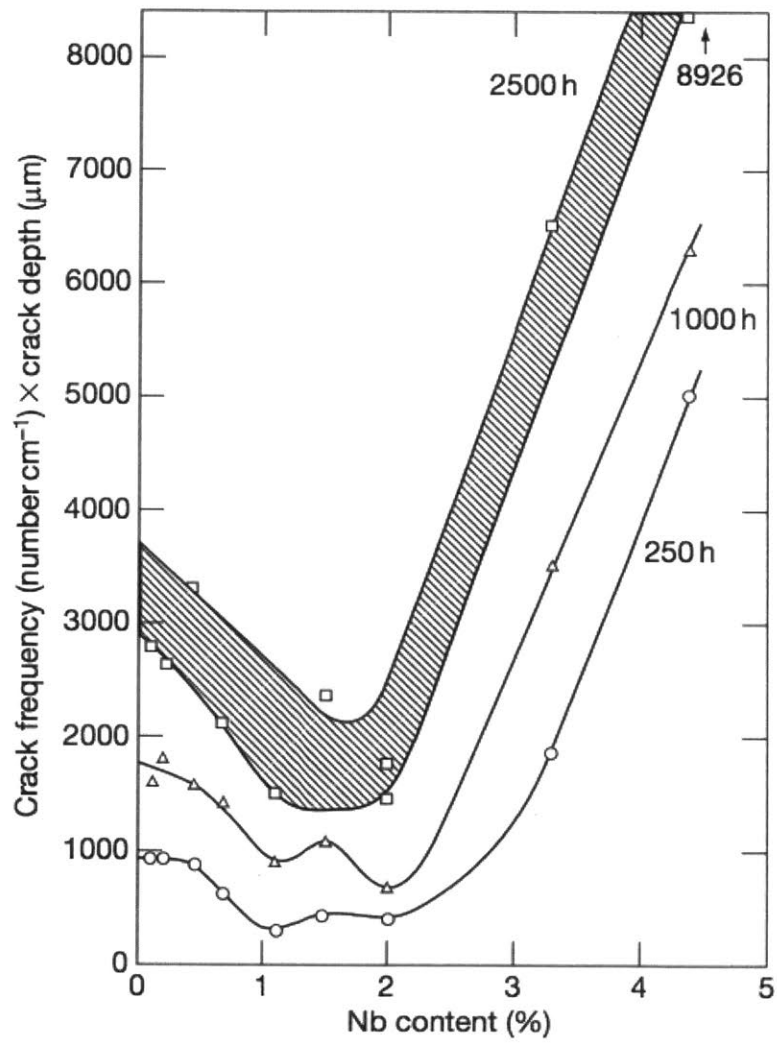
Figure 3: Cracking behavior of Hastelloy N exposed for 260 h at 700 °C to molten-salt breeder reactor fuel salt containing Cr_3Te_4 and Cr_5Te_6. Reproduced from Mc Coy, H. E.; *et al.* Status of materials development for molten-salt reactors, ORNL-TM-5920; ORNL: Oak Ridge, TN, 1978 [6].
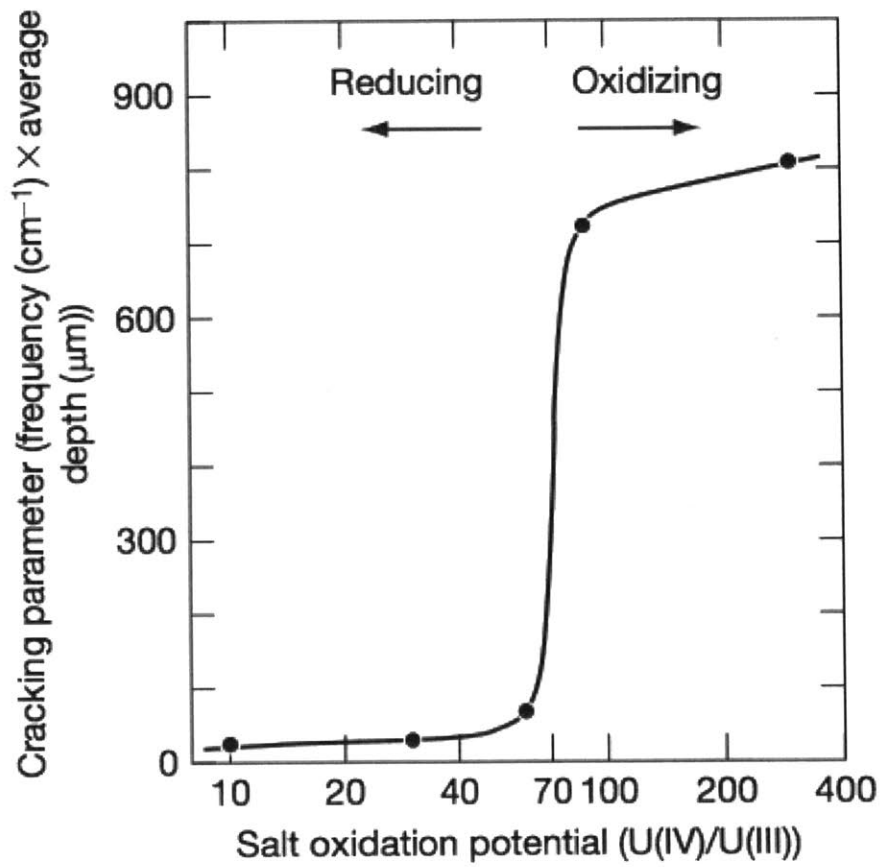
Figure 4: Unit cell of the Σ 5(0 1 2) GB model. The atomic sites are labeled by numbers counted from the GB plane. For clarity, the blue and red balls represent atoms in layers with x = 0.75 (in the paper plane) and x = 0.5 (beneath the paper plane) along the <1 0 0> direction, respectively. The other atoms with x = 0.25 and x = 0 are not shown. The three directions <1 0 0>, <0 2 −1> and <0 1 2> are also shown by arrows [9].
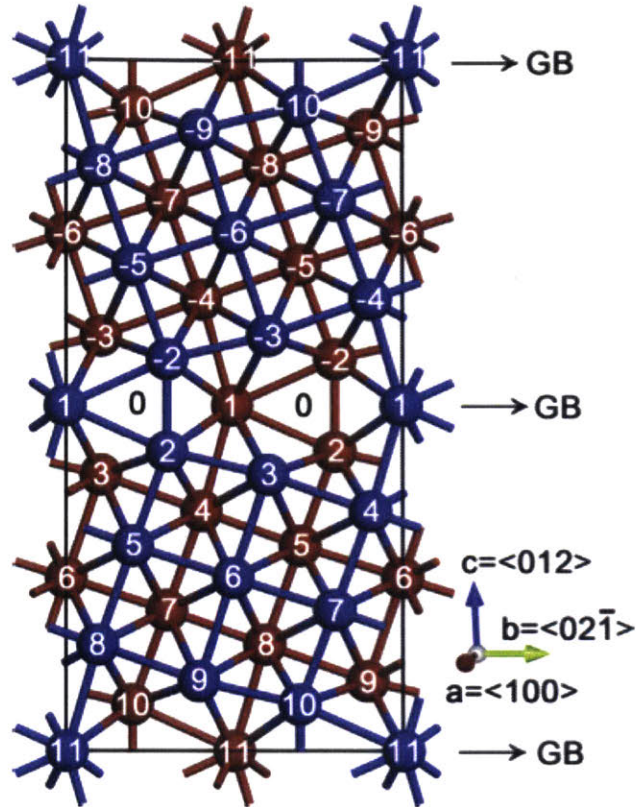
The recent and current research being conducted on the tellurium corrosion problem mainly investigates alloy composition and fuel salt reduction potential. As these newer studies renew the earlier research done on tellurium related IGC, some propose new alloys, new methods for maintaining adequate reduction potentials, as well as some theoretical explanations for the mechanisms by which Te diffuses into GBs.

2.3.1 *First Principles Investigation of Stress Corrosion Cracking*

Using a first-principles approach, researchers at the Shanghai Institute of Applied Physics explored the mechanism of stress corrosion cracking (SCC) due to Te on Hastelloy N. Their calculations confirm earlier results showing that Te prefers to occupy the atomic 1 site at the GB of the alloy, illustrated in Figure 4. Their work goes on to show that concentration of Te in the GB affects expansion. Calculating from first principles the interatomic distances for GBs with various site occupations of Te (see Figure 5), the researchers of this study offer an electronic basis for the relationship between Te concentration in the salt mixture and the embrittlement of the alloy due to GB expansion [9].

Figure 5: Calculated interatomic distances (Å) in the GB region for (a) clean GB, (b) the GB with a Te in layer 1, and (c) the GB with four Te in layer 1. The gray balls represent Ni atoms, and the blue balls indicate Te atoms. [9].

(a) clean GB (b) one Te in layer 1 (c) four Te in layer 1
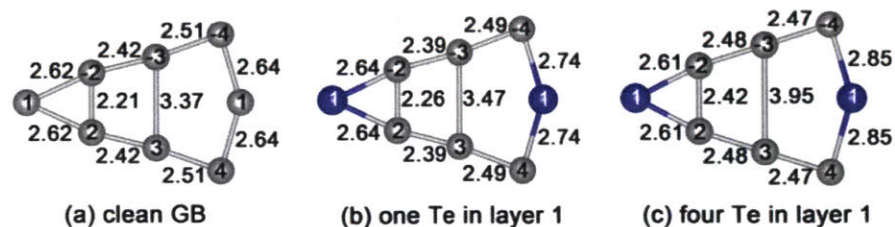
Table 1: Mass fraction of the components in alloys used in the Kurchatov Institute's corrosion tests in molten fluoride salts [2].

	Mass fraction (%)					
Element	Hastelloy N	Hastelloy NM	HN80M-VI	HN80MTY	MoNiCr	HN80MT
Ni	Base	Base	Base	Base	Base	Base
Cr	7.52	7.3	7.61	6.81	6.85	6.9
Mo	16.28	13.6	12.2	13.2	15.8	12.2
Ti	0.26	0.5–2.0	0.001	0.93	0.026	1.6
Fe	3.97	<0.1	0.28	0.15	2.27	
Mn	0.52	0.14	0.22	0.013	0.037	
Nb			1.48	0.01	<0.01	2.6
Si	0.5	<0.01	0.04	0.04	0.13	
Al	0.26		0.038	1.12	0.02	
W	0.06		0.21	0.072	0.16	
Cu	0.02		0.12	0.02	0.016	
Co	0.07		0.003	0.003	0.03	
Zr					0.075	
B	<0.01		0.008	0.003	<0.003	
S	0.004		0.002	0.001	0.003	
P	0.007		0.002	0.002	0.003	
C	0.05		0.02	0.025	0.014	0.02

2.3.2 Corrosion Prevention via Alloy Modification

The research group involved most in alloy modification work of the research reviewed here has taken place at the Kurchatov Institute in Russia. As far back as 2006, they have been investigating alterations to the standard alloy Hastelloy N for their resistance to Te attack. Samples included in one study were dubbed HN80NM-VI, which contained 1 % Nb, HN80MTY, which contained 1 % Al, and MoNiCr, an alloy developed in the Czech Republic that shares similar composition to Hastelloy N. The elemental compositions for these samples are listed in Table 1. The experiment involved loading the samples into a thermal convection loop containing a melt of $58NaF–15LiF–27BeF_2$ and running it through for different temperatures of the melt and different exposure times, ranging from 620 °C to 690 °C and 200 h to 1200 h, respectively [2]. Their findings demonstrated that the samples of HN80MTY and HN80M-VI had an average rate of uniform corrosion of 2 µm–5 µm per year, whereas the average rate for MONICR was over twice as high at 9 µm–19 µm per year [2]. The conclusions the group drew from the results informed them of the corrosion effects of alloying additives [2].

In another study, researchers from the Kurchatov Institute tested an additional sample, HN80MT, and modified the temperatures and exposure times

Figure 6: Microphotographs of HN80MTY alloy specimens surface layer (enlargement × 100) after 500 h exposure to the tellurium containing melt 71.7LiF–16BeF$_2$–12ThF$_4$–0.3UF$_4$. (a) Isothermal tests, T$_{exposure}$=750 °C and (b) nonisothermal tests in loop, T$_{exposure}$=750 °C. Reproduced from Ignatiev, V.V.; Novikov, V.M.; Surenkov, A.I.; Fedulov, V.I. The state of the problem on materials as applied to molten-salt reactor: Problems and ways of solution, Preprint IAE-5678/11; Institute of Atomic Energy: Moscow, USSR, 1993 [6].

(a)   (b)
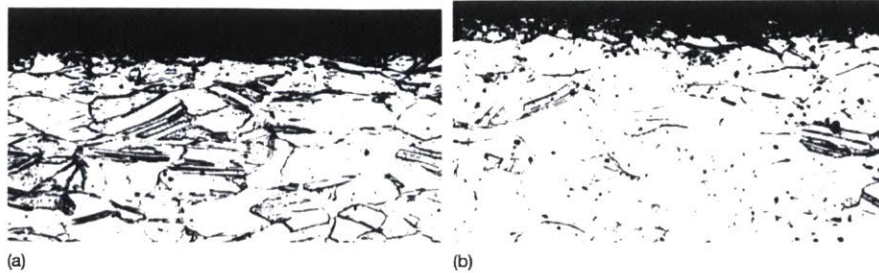
of their thermal convection loop. They tested HN80MT (composition listed in Table 1) and HN80MTY in the loop for 500 h at temperatures ranging from 670 °C–750 °C while including tellurium in an amount specified to be the same that would have been accumulated after 30 y of continuous MSR operation without fission product purification. The maximum corrosion rate of the HN80MTY sample was determined to be 6 μm per year, while the rate for HN80MT was twice as low [3]. The group concluded that the corrosion resistance of both HN80MT and HN80MTY is higher than that of standard Hastelloy N and went on to do tensile testing of the samples. Using a parameter K (representing the product of the number of cracks on a 1 cm length of the longitudinal section of specimens subjected to tensile strain and the average crack depth in microns), they determined that HN80MT is over five times less susceptible to cracking under isothermal conditions at 750 °C than standard Hastelloy N. However, they determined this value to still be insufficient for operation purposes, and concluded that the maximum operating temperature for a reactor using HN80MT must be set to 700 °C [3]. However, they found no IGC either during tensile testing (at 650 °C–800 °C and up to 245 MPa) or in the thermal convection loop at temperatures up to 750 °C when testing HN80MTY [3]. As illustrated in Figure 6, the researchers observed that, in the thermal convection loop, rather than IGC, corrosion proceeded uniformly along grain volume, resulting in a surface layer that stayed in contact with the fuel salt up to a depth of 30 μm. They concluded that HN80MTY is the most promising alloy candidate for a structural material for the MSR capable of withstanding temperatures up to 800 °C [3].

The researchers at the Kurchatov Institute continued their work on tellurium corrosion testing of several alloy samples based on these earlier results. Their experiment involved exposing samples of MONICR, HN80MTY, and HN80M-VI to a melt of 15LiF-58NaF-27BeF$_2$ at 700 °C both with and without a mechanical load of 80 MPa in both dynamic and static flow conditions for times ranging from 100 h–400 h, with a 1.2 V system reduction potential. They found MONICR to be inadequate in its resistance to Te IGC, with a K parameter value over 10,000 pc·μm/cm and cracking observed to depths of 220 μm [6]. However, once again HN80MTY showed most resistance to Te IGC, with a K parameter twice as low as that for HN80M-VI

at 880 pc·μm/cm [6]. They concluded that for their specifications for the design of their MSR concept, called MOSART (MOlten Salt Actinide Recycler and Transmuter), HN80MTY would be a sufficient structural material [6]. In addition, they determined that addition of Re and Y to HN80M-type alloys had only a small effect on mitigating Te IGC, whereas doping with Nb alone exceeded these elements in terms of corrosion resistance. Mn was also found to significantly Te IGC resistance, and the researchers believe additional testing of alloys with various compositions ought to be performed with long exposure times [6].

2.3.3 *Corrosion Mitigation via Electrochemical Technique*

In addition to their work with alloy modifications, the Kurchatov Institute investigated more specifically in another study the effect of the salt mixture's reduction potential on the IGC of the nickel-based container alloy. After testing Hastelloy N specimens at 700 °C in a fuel-salt mixture of 71.7LiF-16BeF$_2$-12ThF$_4$-0.3UF$_4$ for 260 h, they determined that the cracking in the alloy depended on the reduction potential of the salt [4]. They described this reduction potential with the ratio of oxidized uranium to reduced uranium within the mixture, [U(IV)]/[U(III)], and found that keeping this ratio under 60 eliminated the IGC due to Te in the alloy. The results on one such test on Hastelloy N modification HN80MT-VI are shown in Figure 7. K again refers to a parameter used to characterize IGC, defined as number of cracks per centimeter multiplied by their average depth in micrometers [4]. However, if the ratio [U(IV)]/[U(III)] exceeds 500, IGC takes place in all specimens, with HN80MTY showing the most resistance to the corrosion [4].

In another study, the researchers at the Kurchatov Institute also tested another two alloys, HN80MTW (Mo–9.4, Cr–7.0, Ti–1.7, W–5.5) and EM-721 (Cr–5.7, Ti–0.17, W–25.2), in addition to HN80M-VI and HN80MTY, under exposure to molten salt (LiF–BeF$_2$–ThF$_4$–UF$_4$) at temperatures up to 750 °C for 250 h, both with and without mechanical loading up to 25 MPa, allowing the reduction potential in the salt, driven by the ratio of U(IV) to U(III), to vary from 0.5 to 500 Impurities in the salt were measured after the testing, and are listed in Table 2 [4]. The new techniques they employed in this study involved using a new voltametric method for measuring reduction potential of the salt melt during the experiment. They utilized a three-electrode device to measure [U(IV)]/[U(III)] ratio with a molybdenum wire for working and reference electrodes and reactor-grade graphite for the auxiliary electrode. Their device is illustrated in Figure 8 [4]. The results for the sample of HN80MTW, as shown in Figure 9, demonstrated that the alloy also showed no IGC under stress at temperatures up to 750 °C in a reduction potential with U(VI)/U(III) ratio equal to 100 [4]. However, the EM-721 showed minimal resistance to Te IGC [4].

A team of researchers in France studied the effects of Te corrosion on nickel alloy C22 (Ni-22Cr-14Mo-3W-3Fe) in the presence of a molten salt mixture using electrochemistry. They designed a study in which they formed Te vapor by dripping the metal into a crucible containing a model salt mixture of LiF-CaF$_2$-MgF$_2$-ZrF$_4$ and measured the electrochemical dissolution both in the presence and absence of polarization control. After immersing samples for two weeks at 953 K, the results showed that the effects of electrochemical corrosion were significantly mitigated by controlling polarization using electrodes, as seen in Figure 10 [13]. Although alloy C22 is not from

Figure 7: Microstructure of surface layer for HN8oMT-VI alloy (a-c - enlargement x 160) and HN8oMTY (d-f - enlargement x 160) specimens after 250 h exposure in fuel salt: a, d - without loading at 730 °C–735 °C for U(VI)/U(III) = 500; b, e - 25 MPa loading at 730 °C–735 °C for U(VI)/U(III) = 500; c, f - 20 MPa loading at 750 °C for U(VI)/U(III) = 100 [4].

(a) K = 3360 pc×μm/cm

(b) K = 8300 pc×μm/cm

(c) no IGC

(d) K = 1660 pc×μm/cm

(e) K = 1850 pc×μm/cm

(f) no IGC
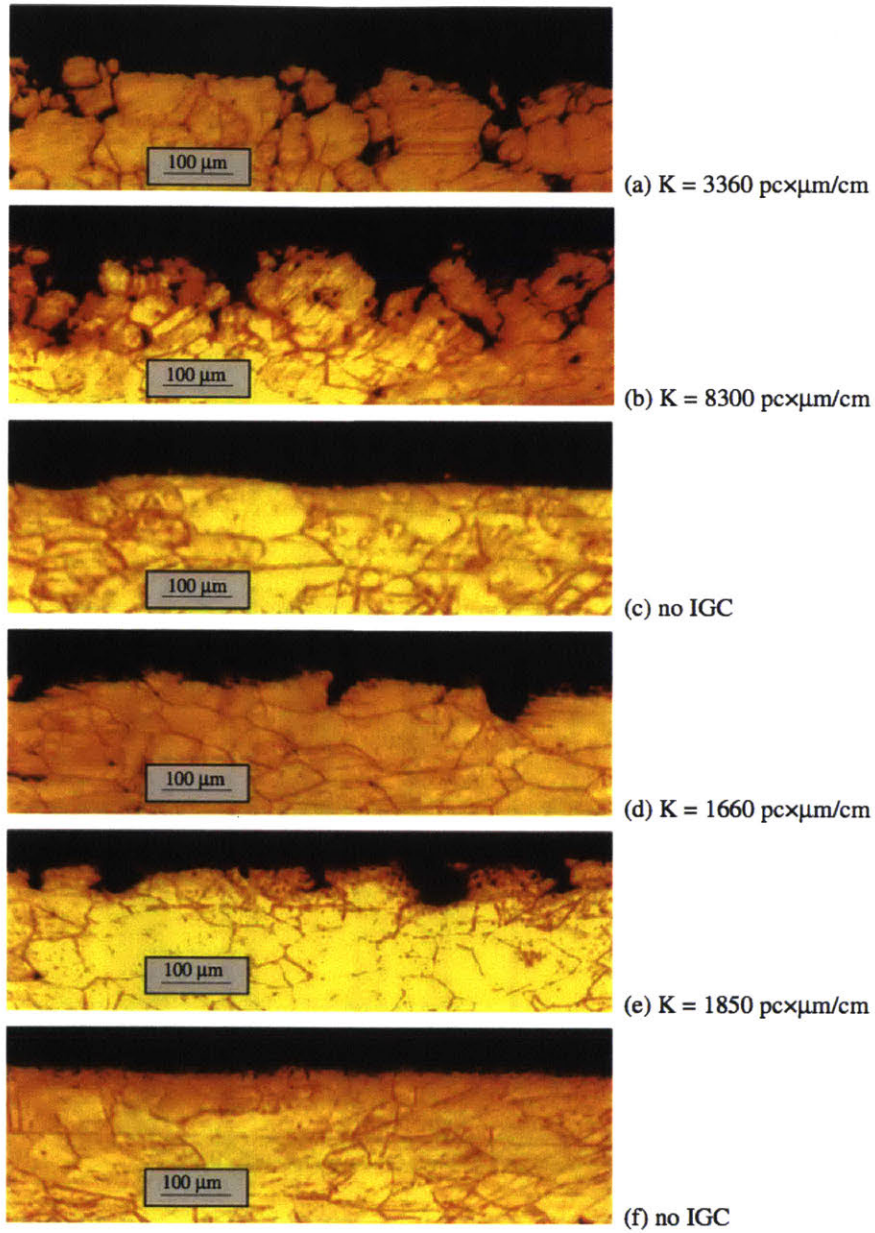
Table 2: Intergranular corrosion tellurium test conditions used in corrosion tests performed at the Kurchatov Institute [4].

Test	$[UF_3 + UF_4]$ (mol%)	$\frac{[U(IV)]}{[U(III)]}$	Temperature (°C)	Impurity content in salt after test (wt%)				
				Ni	Cr	Fe	Cu	Te
I	0.64	0.7	735	0.0034	0.0018	0.054	0.002	0.015
II	2.1	4	735	0.0041	0.0019	0.006	0.0012	0.0032
III	2.1	4	735	0.009	0.0055	0.003	0.001	0.015
IV	2.0	500	735	0.26	0.024	0.051	0.019	0.013
V	2.0	100	750	0.22	0.031	0.065	0.055	0.034

Figure 8: Corrosion facility layout: heaters (1), sampler and level gage of the fuel salt (2), test section with fuel salt (3), tank lid (4), assembling with Ni-base alloy specimens under stress (5), metallic beryllium reducer (6), device for reduction potential measuring (7), container with granulated Cr_3Te_4 (8) [4].
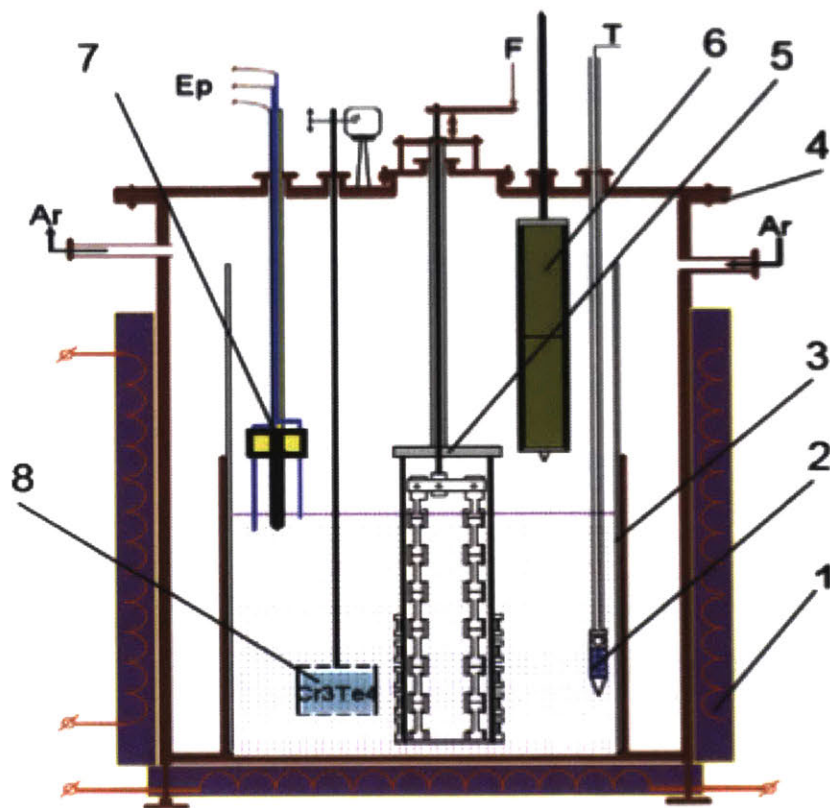
Figure 9: Microstructure of surface layer for HN80MTW alloy (a–c – enlargement ×
160) and EM-721 (d–f – enlargement × 100) specimens after 250 h exposure
in fuel salt: a, d – without loading at 725 °C–735 °C for U(VI)/U(III) = 500;
b, e – 25 MPa loading at 730 °C–735 °C for U(IV)/U(III) = 500; c, f – 20 MPa
loading at 745 °C–750 °C for U(VI)/U(III) = 100 [4].

(a) K = 7060 pc×μm/cm

(b) K = 8400 pc×μm/cm

(c) K = 540 pc×μm/cm

(d) K = 6720 pc×μm/cm

(e) K = 9200 pc×μm/cm

(f) no IGC
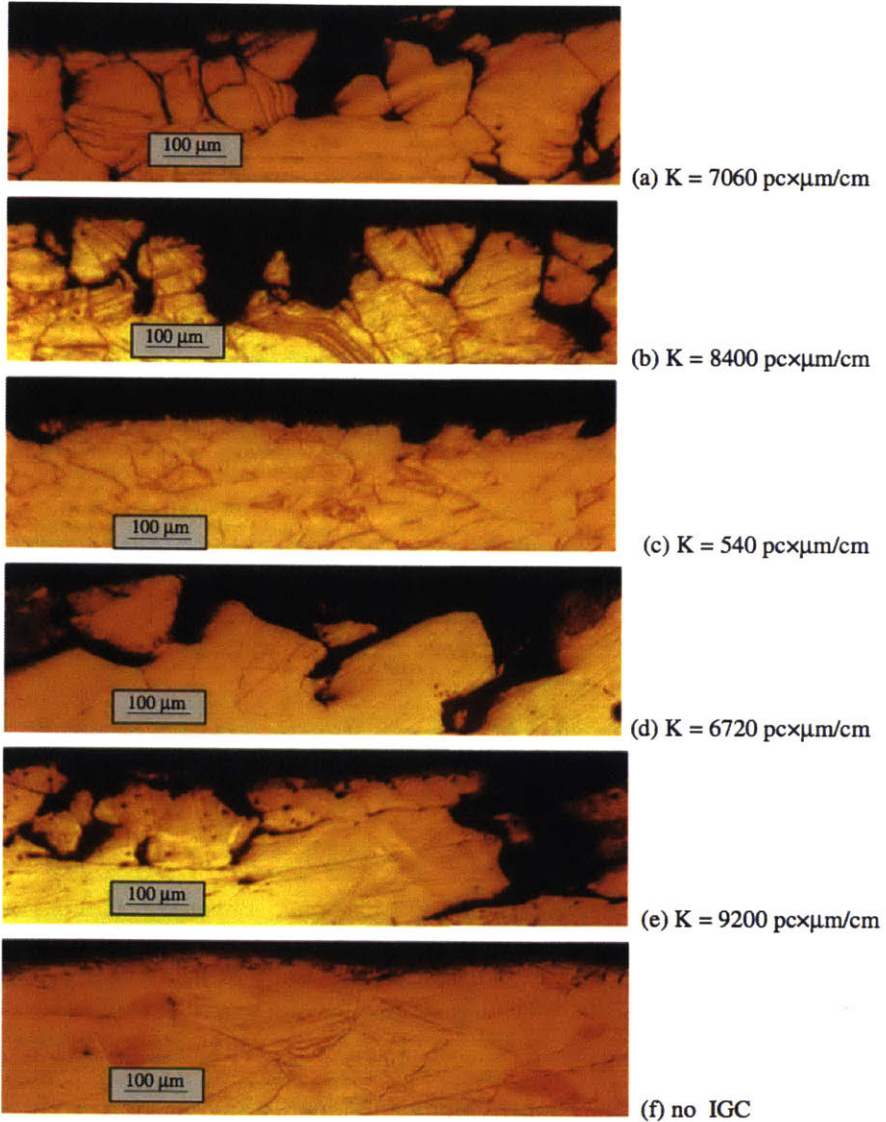
Figure 10: Optical micrographs of Alloy C22 (Ni-22Cr-14Mo-3W-3Fe) immersed for two weeks in LiF-CaF$_2$-MgF$_2$-ZrF$_4$ at 953 K: (a) no Te, no polarization, (b) with Te vapor, no polarization and (c) with Te vapor and polarization at -3.4 V versus F$^-$/F$_2$ (gas) [13].
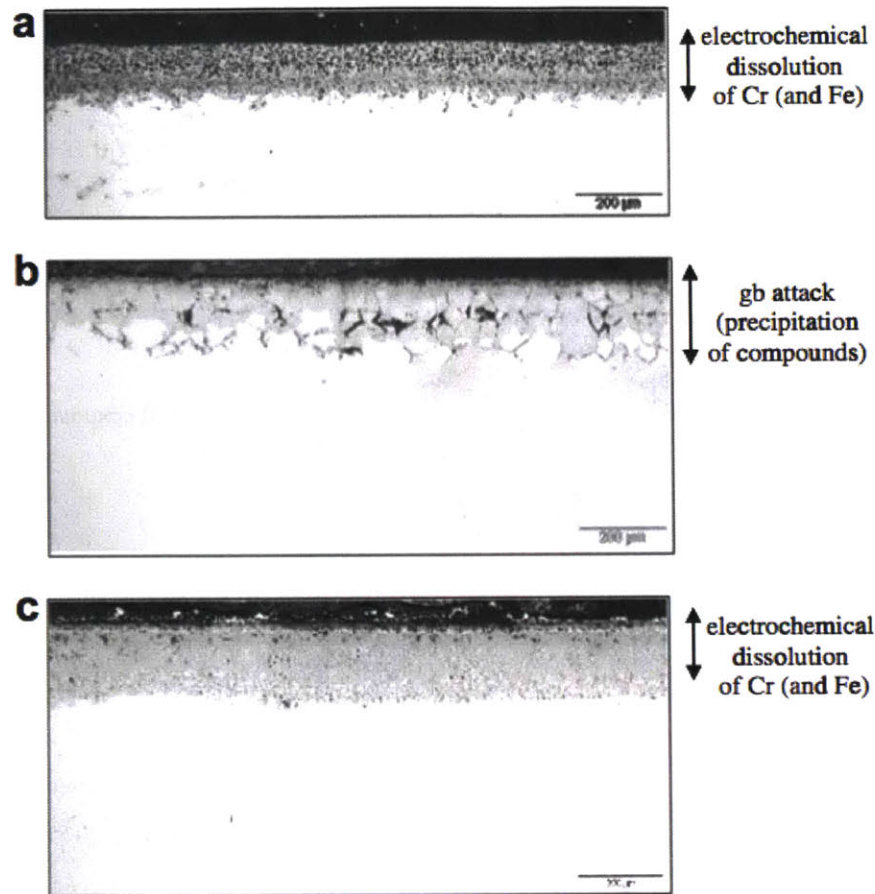
the Hastelloy family, it is a nickel-based alloy that reveals information about Te attack in specific potentials of salt melt.

2.3.4 *Intermetallic Identification in Corroded Alloys*

Researchers from the Shanghai Institute of Applied Physics in China conducted two studies wherein they observed how Te IGC occurred using nickel-based alloys exposed to Te. In the first study, using an alloy with composition Ni-16Mo-7Cr, they deposited Te onto its surface using thermal evaporation at 700 °C. After exposure to Te vapor, they then used X-ray diffraction (XRD-DX2700) and a LEO1530VP scanning electron microscope to observe the surface morphology and identify any reaction products present [1]. They also used a SHIMADZU EPMA-1720H electron probe microanalyzer to determine the distribution of Te inside the sample. Their results showed that the reaction products formed on the surface of the alloy were mostly composed of Ni$_3$Te$_2$, CrTe, and MoTe$_2$ [1]. They note that since many tellurides are unstable, they become sources of Te as it diffuses into the alloy GBs [1]. The researchers furthermore determine using EPMA that most of the Te is enriched on the alloy surface, with little diffusing into the

alloy matrix, as illustrated in Figure 11 [1]. However, the thickness of the layer of Te on the alloy surface significantly increases with Te concentration, while some intergranular diffusion occurs at higher concentration as well [1]. Furthermore, the research group ran tensile tests on alloy samples after subjecting them to constant stress for 24 h. Again using a parameter K to compare cracking characteristics, they observed that Te concentration had little effect on cracking, whereas it does have an effect on tensile properties, causing the alloy to have shorter elongation to fracture and lower ultimate tensile strength [1].

In another study, researchers from the Shanghai Institute used EPMA and transmission electron microscope (TEM) to characterize tellurium corrosion on another nickel-based alloy with composition Ni-16Mo-7Cr-4Fe. After annealing a sample of the alloy at 800 °C for 100 h in Te vapor, they examined it using EPMA, identifying surface reaction products CrTe and Ni_3Te_2 [14]. They make note of the fact that despite the assumed theory that Te IGC in Ni-based alloys is caused by brittle tellurides forming at GBs, no such intergranular tellurides had yet been observed prior to their work [14]. They theorize that CrTe, a brittle intermetallic, forms at GBs and within the intergranular carbide matrix, both embrittling the sites of formation and preventing GBs from sliding and allowing cracks to begin [14].

3 METHODS

3.1 Overview

To obtain a corrosion rate of tellurium into the grain boundaries of specific alloys and to identify any reaction products contributing to intergranular corrosion of the alloy samples, four selected alloys were lowered within a heated, sealed autoclave via nickel rods until immersed in molten FLiNaK salts at 700 °C for 50 h, 100 h, and 150 h. To compare corrosion rates of tellurium against a control and to properly identify telluride reaction products, two separate tests were run for each time duration on each alloy sample: one in FLiNaK salts containing only the reduction potential agent europium(III) fluoride (EuF), and another in FLiNaK salts containing both the reduction potential agent EuF and nickel(II) telluride (NiTe). The samples, once removed from immersion in molten salts, were collected, cut, polished, and examined using scanning electron microscopy (SEM) and energy-dispersive x-ray spectroscopy (EDS).

3.2 Sample Selection and Preparation

3.2.1 *Motivation for Alloy Selection*

Four sample alloys were chosen to test for corrosion in a molten salt environment. These alloys were Hastelloy N, Nickel 201, Incoloy 800H, and 316L Stainless Steel. Hastelloy N was chosen to compare with previous work done using this alloy on the MSRE at ORNL in the 1970s. Nickel 201 was chosen to understand a baseline level of corrosion in the balance material of the corrosion-resistant nickel superalloys. Furthermore, as it is a highly corrosion-resistant alloy [15], if not a structural one, its use as a liner to the inside of cheaper, more structural alloys may in the future prove to be a viable method for building a molten salt reactor. Incoloy 800H was chosen

Figure 11: Te distribution of alloy aged with different Te contents at 700 °C for 100 h: (a) 1 g m^{-2}, (b) 4 g m^{-2}, (c) 8 g m^{-2}, (d) 10 g m^{-2}, (e) 20 g m^{-2} [1].
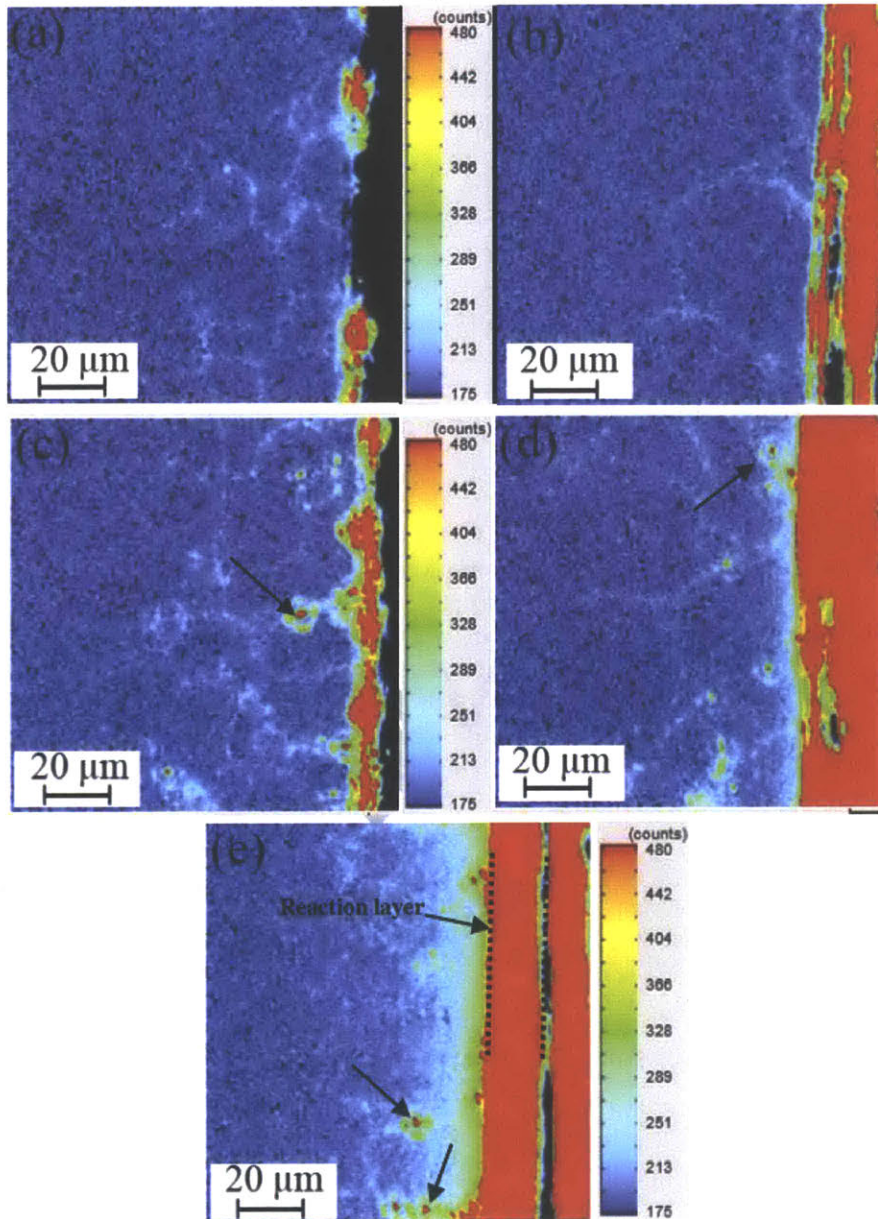
Table 3: Dimensions of the sample alloys coupons measured using a digital calibers prior to preparatory polishing and immersion in molten FLiNaK salts.

Alloy	Length (mm)	Width (mm)	Depth (mm)
Hastelloy N	20.10	10.40	1.52
Incoloy 800H	20.10	10.40	3.17
Nickel 201	20.10	10.40	6.73
316L Stainless Steel	20.10	10.40	6.23

for its potential as a nuclear molten salt reactor structural alloy due to its high corrosion resistance, strength, and workability [16]. Lastly, 316L Stainless Steel, being a commonly used corrosion-resistant structural steel [17] and cheaper than nickel-based superalloys, was chosen to examine if it is of sufficient corrosion resistance to consider as a structural material in future work on MSRs.

3.2.2 Alloy Preparation for Immersion in Salt

Sample coupons of each alloy were cut using electrical discharge machining (EDM). The thickness of each coupon corresponded with the thickness of the alloy sheet stock from which it was cut. A summary of the dimensions of the coupons can be found in Table 3. These dimensions were chosen for each coupon to fit inside the nickel crucibles that were custom made for the experiment (see Figure 12, Appendix A) with an inner diameter of 0.731 in.

Once cut to size, each coupon was given two 1.0 mm holes using EDM through which 99.98 % nickel wire was threaded to tie the coupons to nickel rods for lowering into molten salt during testing. One face of each coupon was polished using a Buehler MetaServ®250 with Vector®Power Head. The steps used to polish each coupon prior to testing are outlined in Table 4. Once polished, each sample was cleaned using a two-step process in a sonic bath: First, they were sonically bathed for a minute in a beaker containing ethanol, and then each was transferred to a beaker containing acetone and sonically bathed for another minute before removal and drying. The clean sample coupons were stored in resealable plastic bags.

3.2.3 FLiNaK Salt Mixture and Preparation

To prepare the salt for the immersion of samples at high temperature, it was first necessary to mix FLiNaK in proper ratios from the individual fluoride compounds lithium fluoride (LiF), sodium fluoride (NaF), and potassium fluoride (KF). These ratios can be found in Table 5. Furthermore, the reduction potential agent EuF was added to the mixture of fluoride salts in order to control the potential in a way that would more realistically imitate a controlled fuel salt under normal operation in a reactor than pure FLiNaK alone. Adding a reduction potential agent such as EuF can affect the corrosion rate of materials exposed to the salts due to how strongly fluorides will tend toward reduction or oxidation, and it may be used in future as a method to mitigate structural damage in molten salt reactors [19].

Two batches[1] of a control salt were mixed without the addition of any NiTe, while one batch of a test salt was mixed with the addition of NiTe.

---

1 The second batch of the control salt was prepared in response to the loss of two samples during the first corrosion test. Using the second batch of control salt, replacement samples for the two lost samples were included in the second corrosion test.

Table 4: A summary of the polishing steps taken to prepare each alloy sample coupon for immersion into molten FLiNaK during corrosion tests. These steps as outlined were based on information found in Buehler® Sum-Met™[18]. Because the samples were being prepared for corrosion in salt, and not for imaging, the polishing steps listed here were not followed precisely, but rather they represent the basic process followed for each sample as it was taken to a polished finish on one side. Note that up to eight of each sample coupon were polished on a sample holder at once, so an exact value for load/specimen cannot be provided. Furthermore, of the four alloys polished at this stage, only 316L Stainless Steel was polished through steps V and VI. The Hastelloy N, Nickel-201, and Incoloy 800H samples appeared adequately polished without scratches visible to the naked eye after steps I–IV.

Step	Surface	Abrasive	Grit	Load (N)	Base Speed (rpm)	Relative Rotation	Time (min:sec)
I	Car-bimet	SiC	120	40	200	Comp.	15:00
II	Car-bimet	SiC	240	40	200	Comp.	10:00
III	Car-bimet	SiC	400	40	200	Comp.	10:00
IV	Car-bimet	SiC	800	40	200	Contra	5:00
V	Car-bimet	SiC	1200	40	200	Comp.	5:00
VI	Car-bimet	SiC	1200	40	200	Contra	5:00

The specific compositions of each batch are laid out in Table 6. Each of these three batches of mixed powdered salts was then placed inside of a glassy carbon crucible and melted at a temperature held above the eutectic point of FLiNaK, 454 °C, in a sealed autoclave under argon cover gas for several hours. Glassy carbon was chosen both for its ability to withstand high temperatures and for the ease of removal of salt from its surface. Once fully cooled, each batch of salt was removed from its glassy carbon crucible and broken and ground roughly into pieces to prepare it for placing in smaller nickel crucibles during corrosion testing.

3.3 Experimental Setup

The experiment was designed to test up to fifteen samples at once, immersed in molten FLiNaK salt at 700 °C, for durations of 50 h, 100 h, or 150 h. A sim-

Table 5: Composition of FLiNaK salt by mass fraction [20]. Note that in Table 6 the total mass of each batch of mixed salt is greater than 100 g. However, the masses of the LiF, NaF, and KF in each batch were chosen to total 100 g as closely as possible, such that the mass fraction of each salt in the standard composition of FLiNaK given here can be compared easily to the mass in grams of each salt in all mixed batches.

Salt	Mass Fraction (%)
LiF	29
NaF	12
KF	59

Table 6: Compositions of batches of FLiNaK mixed from the powder form of LiF, NaF, and KF salts, with powder form EuF added as a reduction potential agent. Batches I and II were used to prepare salt for testing a set of control samples and contained no added NiTe, while Batch III was used to prepare salt for testing corrosion in the presence of Te, and contained added NiTe. The added NiTe was crushed from 10 mm and down lump form into a powder with a mortar and pestle.

Batch	Salt	Purity (%)	Mass (g)	Mass Fraction (%)
I.	LiF	99.99	29.2123	27.8233
	NaF	99.995	11.6870	11.1313
	KF	99.0	59.0886	56.2791
	EuF	99.98	5.0042	4.7663
II.	LiF	99.99	29.2131	27.8240
	NaF	99.995	11.6864	11.1307
	KF	99.0	59.0898	56.2801
	EuF	99.98	5.0030	4.7651
III.	LiF	99.99	29.2123	27.7847
	NaF	99.995	11.6870	11.1159
	KF	99.0	59.0886	56.2009
	EuF	99.98	5.0042	4.7596
	NiTe	99.9	0.1460	0.1389

plified diagram of the experimental setup is illustrated in Figure 12. Fifteen crucibles with threaded bases were screwed into an annular baseplate. The baseplate and each crucible were custom machined from Nickel 201 alloy pipe and plate (see Appendices A and B.2). The threading was a design feature intended to prevent tipping during corrosion testing when samples would be lowered via nickel rods into the salt-filled crucibles within a sealed system. The baseplate sat inside a metal autoclave, propped up on scrap pipe to add height to the crucibles relative to the top of the autoclave as needed during setup to allow for proper alignment with sample coupons. Each sample alloy coupon was tied to a nickel rod via 99.98 % nickel wire so that it could be safely lowered into its respective crucible containing molten FLiNaK salt during testing and retracted again before cooling and hardening of the salt.

The autoclave sealed at the top via a stainless steel flange that had been custom machined to include through-welded stainless steel pipe. Sixteen of the welded pipe additions also had tightening knurled nuts welded to their ends such that a Nickel 201 alloy rod could be lowered down through each one and tightly held in place with a rubber o-ring to seal the inside of the autoclave from outside air. Stainless steel tubing was also welded to the top flange of the autoclave to allow for an argon cover gas inlet and outlet, as well as for a thermocouple to be inserted into the system. Each of these tubes sealed via Swagelok tube fittings. More detailed design specifications for the construction and customization of the experimental setup can be found in Appendix A.

The autoclave containing the Nickel 201 crucibles was placed within a Mellen CS Crucible furnace. Its gas inlet was connected to a supply of argon gas, set at approximately 15 psi inlet pressure via argon gas regulator, from either ultra-high-purity Grade 5 liquid argon, industrial grade liquid
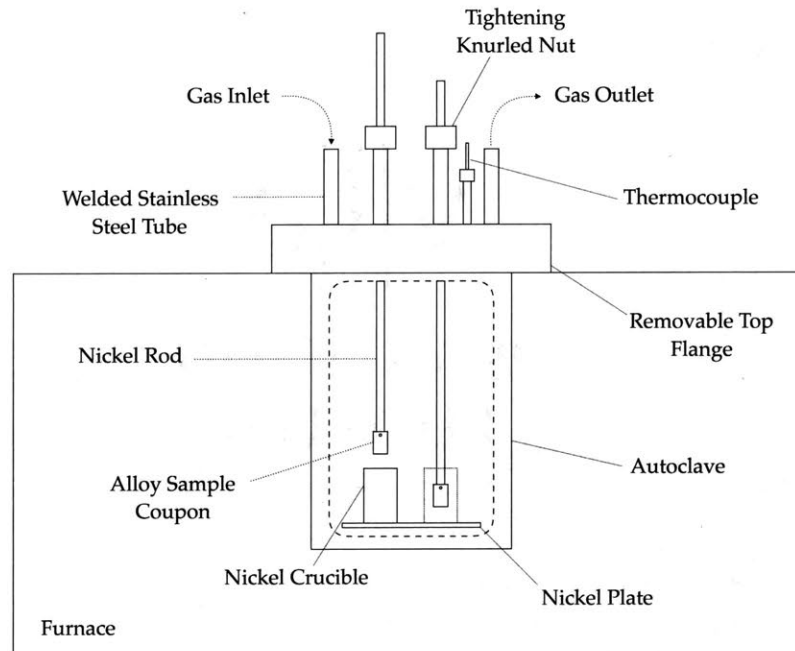
Figure 12: Diagram of experimental setup. The autoclave sealed via a 10 in MDC Vacuum flange with copper gasket, customized to include sixteen welded stainless steel tubes extending from the top and outfitted with tightening knurled nuts that allowed for rods to be lowered through each pipe at variable heights during corrosion tests while maintaining a tight seal from outside air. These rods were used to immerse each sample coupon into its respective crucible containing molten FLiNaK during corrosion testing. A gas inlet and outlet were also machined to the top flange using stainless steel tubing, as well as a tube for the insertion of a thermocouple.
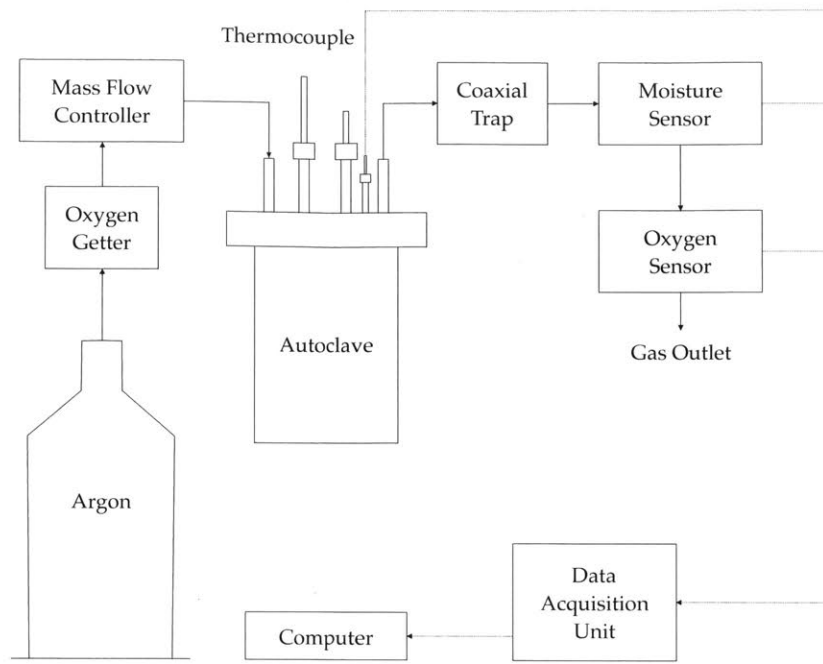
Figure 13: Diagram of experimental sensors and argon cover gas flow. Argon was delivered as a cover gas throughout the interior of the sealed autoclave during corrosion testing. A mass flow controller delivered the argon at approximately 5 SCFH. Before entering the gas inlet to the autoclave, the argon was purified of oxygen via an oxygen getter outfitted with a titanium cartridge. After the argon flowed out of the autoclave, moisture and oxygen concentration data were collected and logged via a data acquisition unit. The outlet cover gas flowed through a coaxial trap in an effort to prevent fluoride salt vapors from contaminating downstream sensors. Meanwhile, a thermocouple also connected to the data acquisition unit delivered data on the interior air temperature of the autoclave.

argon, or compressed Grade 4.8 argon gas, depending on availability during a corrosion test. The argon gas was sent through a Centorr Model 2A Inert Gas Purifier to trap any oxygen present before flowing through a Sierra Instruments SideTrak® 840 mass flow controller that was calibrated within two years of these corrosion tests. This mass flow controller was connected to a Sierra Instruments FloBox™ 951/954, which digitally regulated the mass flow of the argon to approximately 5 SCFH.

After flowing through the autoclave, the argon then flowed through a coaxial trap as a precautionary measure against salt vapors contaminating downstream sensors. It then flowed through a Teledyne Analytical Instruments Model 8800T Trace Moisture Analyzer and a Delta F Platinum Series oxygen analyzer prior to outlet. Data from each of these sensors was collected via a Keysight 34970A Data Acquisition/Switch Unit connected to a logging computer. Meanwhile, temperature data from a K-type thermocouple sheathed in Incoloy 600 was collected via the Keysight 34970A Data Acquisition/Switch Unit and logged.

3.4 Test Procedure

3.4.1 First Salt Corrosion Test

The first corrosion test included twelve sample coupons immersed in Batch I of the FLiNaK salt (see Table 6). The autoclave was sealed with roughly ground Batch I FLiNaK salt placed in each of twelve crucibles and with the sample coupons aligned with each crucible such that they could be lowered into the salt once it had melted during testing. The furnace was then switched on and the interior of the autoclave was brought up to 700 °C as read via the inserted thermocouple. Once the temperature was sitting stably at 700 °C and the oxygen and moisture levels had plateaued to their respective minimums, all nickel rods with attached sample coupons were lowered into the salt-containing crucibles.

One each of Hastelloy N, Incoloy 800H, Nickel 201, and 316L Stainless Steel was held in salt for 50 h. Likewise one of each alloy was held in salt for 100 h and for 150 h. At the end of each time duration, the nickel rods attached to those four samples were drawn upward within the autoclave to remove the sample from the molten salt while any remaining samples continued to corrode for longer durations until all were complete. Once all samples had been drawn up out of the salt, the furnace was switched off and the autoclave was allowed to cool under argon cover gas. The samples were then removed once the system had returned safely to room temperature. Upon removal from the first corrosion test, it was discovered that two sample coupons had broken off from their respective nickel rods and had been lost in the hardened salt. These samples were noted and included as supplemental samples in the next corrosion test round.

During this first corrosion test, several unexpected losses in argon cover gas pressure resulted in some oxygen contamination in the system as the argon supply was switched out. These spikes in oxygen concentration can be seen in Figure 14. As the longest of these lasted approximately 3 h, it is important to note their presence, though the sample's full immersion in molten salt may have helped to prevent a temporary increase of oxygen concentration from severely affecting corrosion rate. The temperature, and moisture levels for this first corrosion test are illustrated in Figures 15 and 16, respectively.

3.4.2 Crucible Cleaning Between Corrosion Tests

To preserve the integrity of the salt composition of Batch III (see Table 6) prior to its use in the second corrosion test, a thorough cleaning of the nickel crucibles was undertaken using a combination of heat, acid wash, and abrasion techniques. First, each crucible was held over a bunsen burner flame for several minutes until its solid FLiNaK contents were molten and able to be poured into a waste receptacle. Next, FLiNaK residue that adhered to the nickel crucibles during this melting and disposal process was dissolved in a 1.0 M $Al(NO_3)_3$ solution with the aid of heat and agitation from a laboratory hotplate. Remaining surface residue was then finally polishing away using a rotary tool equipped with steel wire brushes. A final cleaning in a sonic bath of acetone followed by ethanol for a minute each left the crucibles ready for the next corrosion test.

Figure 14: Concentration of oxygen in the argon cover gas inlet to the autoclave, measured in parts per million, during the first corrosion test of alloy samples in FLiNaK salt without added NiTe. The total 150 hr duration of the corrosion test is denoted between the dashed lines. The spikes in the oxygen concentration during this corrosion test were due to unexpected loss of argon pressure, which was corrected in subsequent corrosion tests.

Figure 15: Temperature measured in the autoclave during the first corrosion test of alloy samples in FLiNaK salt without added NiTe. The total 150 hr duration of the corrosion test is denoted between the dashed lines.
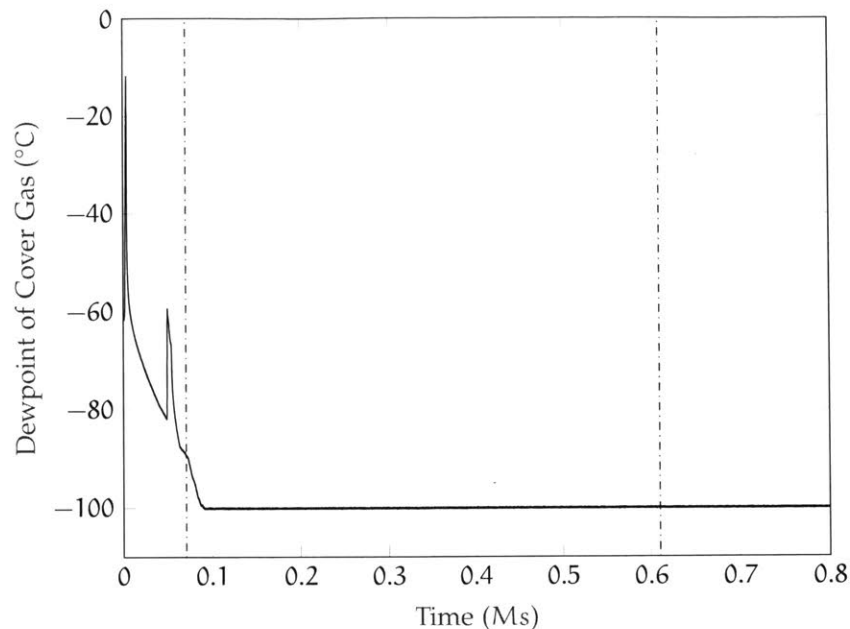
Figure 16: Moisture measured in the argon cover gas inlet to the autoclave, measured by dew point (°C), during the first corrosion test of alloy samples in FLiNaK salt without added NiTe. The total 150 hr duration of the corrosion test is denoted between the dashed lines.

3.4.3 Second Corrosion Test

The procedure for the corrosion test followed the same steps as those for the first corrosion test (see Section 3.4.1), but Batch III (see Table 6) salt was used for the set of twelve alloy samples being immersed in it to test for tellurium corrosion rate and products. To make up for the two samples lost in the first corrosion test, two additional samples were included and lowered into spare crucibles containing salt from Batch II (see Table 6), another batch of FLiNaK salt mixed without added NiTe to match the composition of Batch I as closely as possible. The oxygen, temperature, and moisture levels for this second corrosion test are illustrated in Figures 17 18, and 19, respectively. Two samples broke off from their respective nickel rods during the second corrosion test, so a supplemental third corrosion test was planned to accommodate these samples.

3.4.4 Third Corrosion Test

To avoid the lengthy cleaning procedure for the nickel crucibles in preparation of an unexpected third corrosion test, two new crucibles were fashioned from 99 % purity nickel foil and tested for liquid-tightness with acetone. Subsequently, the procedure for the third corrosion test followed that of the first and second tests, with two notable exceptions.

First, only two sample coupons were tested. A Hastelloy N sample coupon was immersed into Batch II salt, and a Nickel 201 sample was immersed into Batch III salt, for 100 h each.

Second, to contain any potential spills of molten salt arising from leaks in the thin nickel foil crucibles during testing, each crucible was placed within a larger glassy carbon crucible, which was then placed onto the annular nickel baseplate resting on the bottom of the autoclave. While the base-
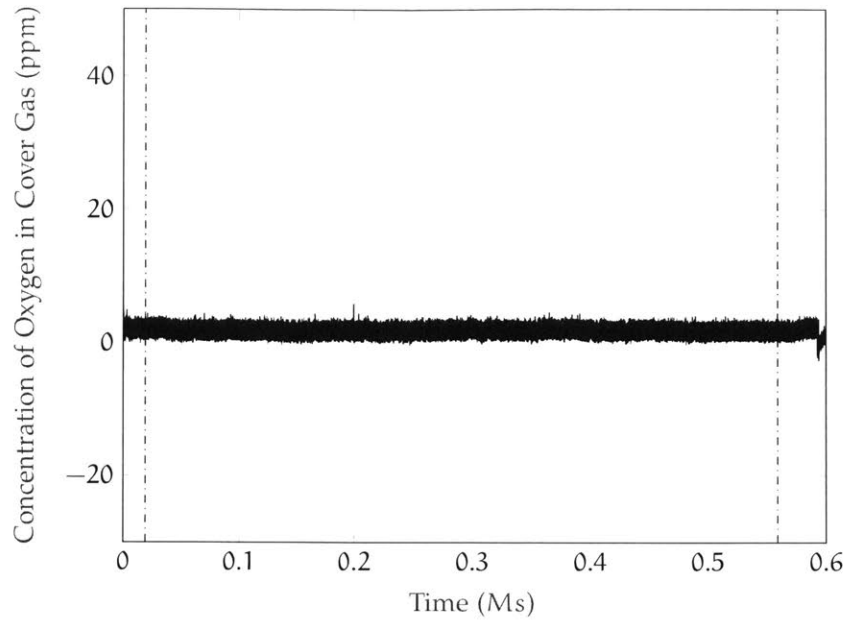
Figure 17: Concentration of oxygen in the argon cover gas inlet to the autoclave, measured in parts per million, during the second corrosion test, including alloy samples in FLiNaK salt with and without added NiTe. The total 150 hr duration of the corrosion test is denoted between the dashed lines.
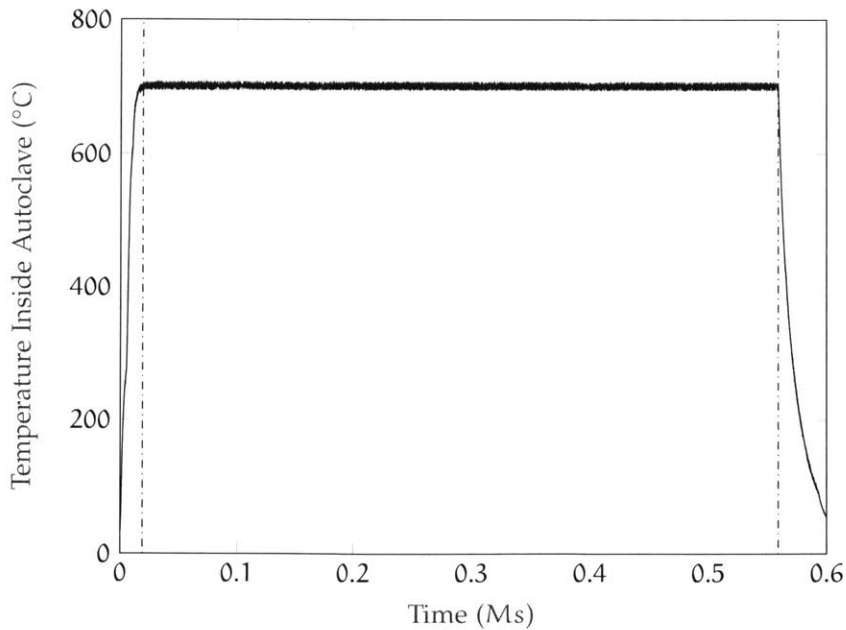
Figure 18: Temperature measured in the autoclave during the second corrosion test, including alloy samples in FLiNaK salt with and without added NiTe. The total 150 hr duration of the corrosion test is denoted between the dashed lines.
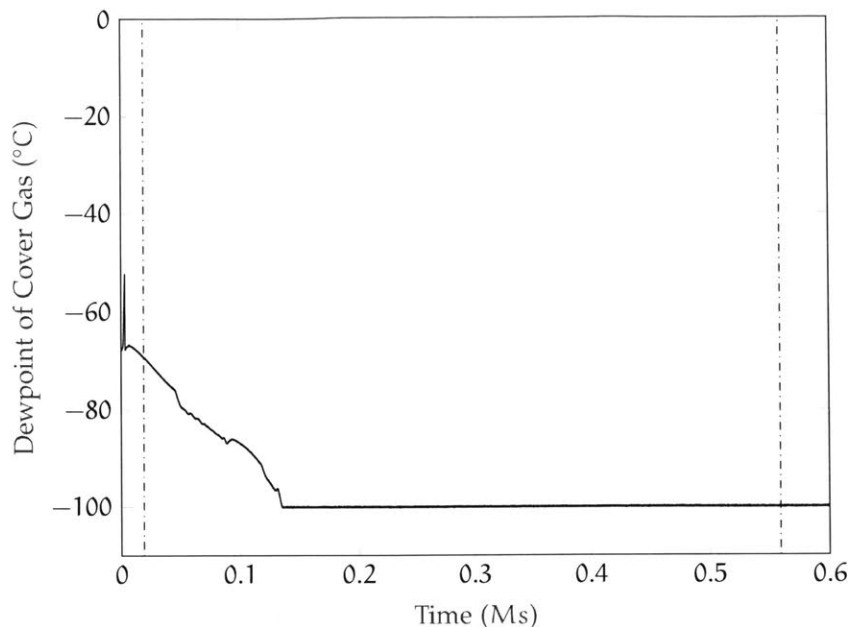
Figure 19: Moisture measured in the argon cover gas inlet to the autoclave, measured by dew point (°C), during the second corrosion test, including alloy samples in FLiNaK salt with and without added NiTe. The total 150 hr duration of the corrosion test is denoted between the dashed lines.

plate was propped onto scrap pipe during the first and second corrosion tests to allow for easier alignment with sample coupons during setup, no such alignment was necessary for only two widely-formed foil crucibles, and the scrap pipe was not used during the third corrosion test. This lower placement within the autoclave may have resulted in greater heat conduction through the bottom of the metal autoclave in contact with the nickel baseplate.

When the samples were removed from the cooled autoclave after the third corrosion test, it was discovered that the nickel foil crucibles had in fact leaked some molten salt into the glassy carbon crucibles, but enough had stayed within each foil crucible that consistent immersion throughout the duration of the test appeared to have been successful.

The oxygen, temperature, and moisture levels for this third corrosion test are illustrated in Figures 20 21, and 22, respectively.

3.5 Alloy Sample Polishing and Preparation for Imaging

After being removed from the corrosion tests, each sample was sectioned on a Buehler® IsoMet Low Speed Saw. Each section was then mounted in EpoMet, a mineral SiO_2 filled epoxy thermoset, using a Struers PrestoPress-3. The orientation of each sectioned sample was chosen such that the smooth, pre-test-polished corrosion layer would lie perpendicular to the plane of polishing and thus be well revealed at its edges under an SEM. The steps used for polishing each alloy can be found in Tables 7, 8, and 9. Following polishing, each mounted sample was rinsed well with deionized water and immediately dried using compressed air in an effort to prevent salt crystallization buildup on the surface to be imaged. The samples were then stored in sealed jars containing Drierite, a desiccant composed of $CaSO_4$, in
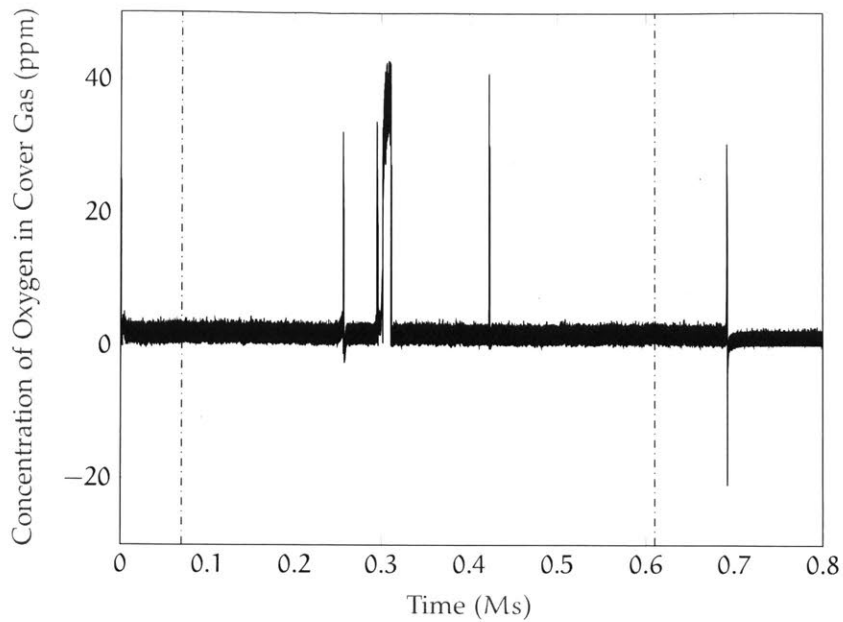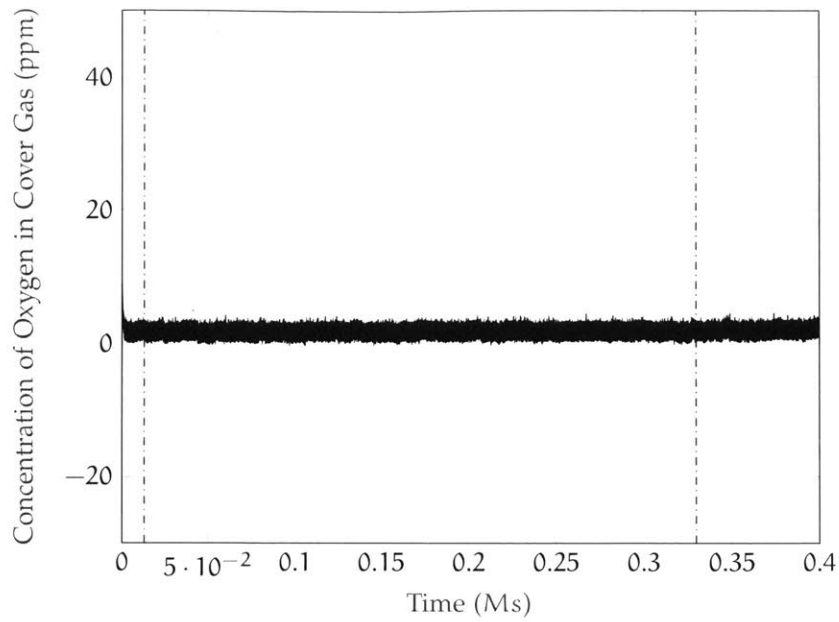
Figure 20: Concentration of oxygen in the argon cover gas inlet to the autoclave, measured in parts per million, during the third corrosion test, including alloy samples in FLiNaK salt with and without added NiTe. The total 150 hr duration of the corrosion test is denoted between the dashed lines.
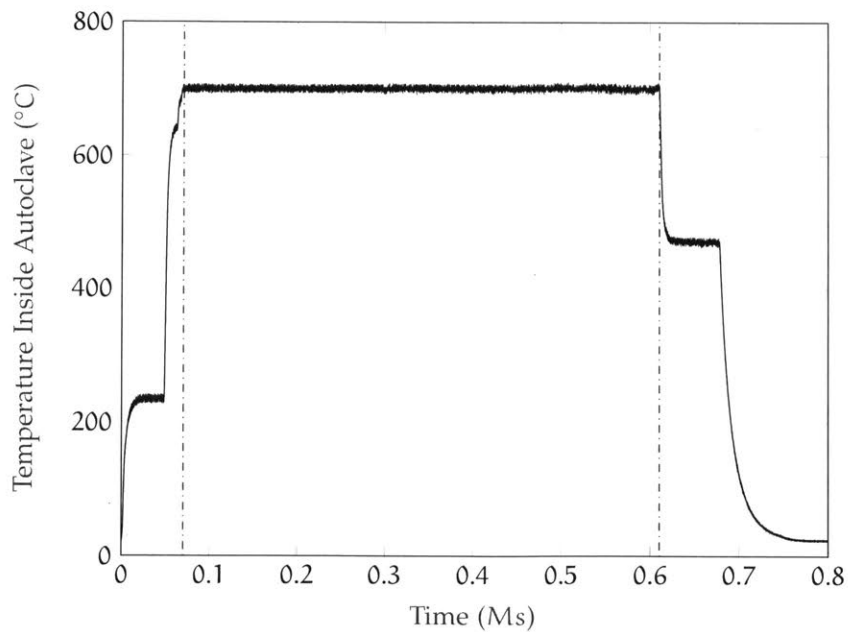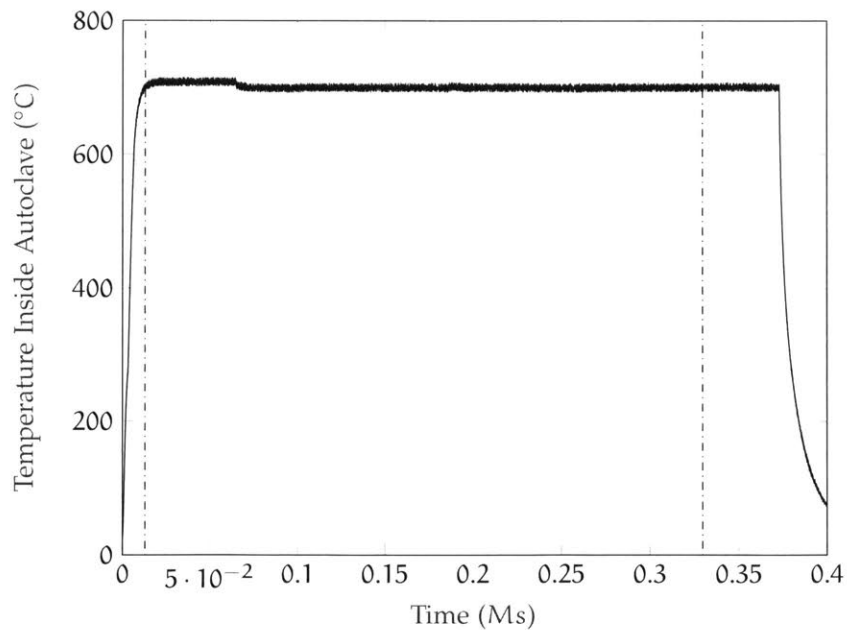

Figure 21: Temperature measured in the autoclave during the third corrosion test, including alloy samples in FLiNaK salt with and without added NiTe. The total 150 hr duration of the corrosion test is denoted between the dashed lines.
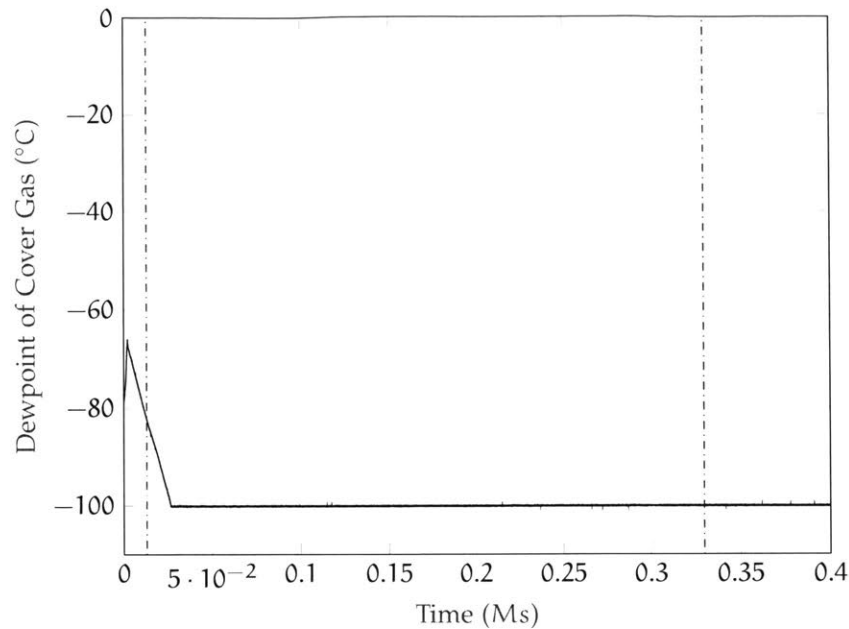
Figure 22: Moisture measured in the argon cover gas inlet to the autoclave, measured by dew point (°C), during the third corrosion test, including alloy samples in FLiNaK salt with and without added NiTe. The total 150 hr duration of the corrosion test is denoted between the dashed lines.

order to keep them dry and safe from scratches. Finally, each sample was coated with 10 nm of gold using an evaporator in order to prevent electron charging and aid with imaging using the SEM.

3.6 Alloy Sample Imaging Using Scanning Electron Microscopy

Each sample was imaged using a JEOL JSM-5910 SEM equipped with a Bruker EDX system for elemental analysis and mapping. The software used to perform the elemental analysis was Esprit 2.0 Microanalysis Software by Bruker. Images of varying magnification were taken of each sample, with a consistent working distance, spot size, and voltage among sample set. A 300 s or 600 s line-scan of each 150 h sample was performed using the Bruker EDX system, as well as one EDS map of the 150 h Hastelloy N sample immersed in FLiNaK containing NiTe. In addition, line-scans of a sample of NiTe lump and a sample of the Batch III salt (see Table 6) were performed.

During inspection under the SEM, an effort was made to image the edge of the sample which was polished prior to being corroded in molten salt to give as uniform a baseline edge as possible against which to compare corrosion depth and features. In samples where the polished edge was indistinguishable from the unpolished edge, or where there was so much surface salt crystal growth from FLiNaK salt embedded in the EpoMet that it was difficult to image the polished edge, an image was taken from another area with as flat an apparent baseline edge as possible.

Table 7: The polishing steps followed for the 316L Stainless Steel samples after corrosion testing. Each sample was mounted in EpoMet, a mineral SiO_2 filled epoxy thermoset, and polished on a Buehler MetaServ®250 with Vector®Power Head. The steps chosen were adapted from the Buehler® *Sum-Met*™, though each step was repeated or adjusted in response to the polishing progression of the samples [18].

Step	Surface	Abrasive	Load (lbs.)	Base Speed (rpm)	Relative Rotation	Time (min:sec)
I	Carbimet	400 grit SiC	6	150	Contra	Plane
II	UltraPol Cloth	9-µm MetaDi Supreme Diamond Suspension	6	150	Comp.	5:00
III	TriDent Cloth	3-µm MetaDi Supreme Diamond Suspension	6	150	Comp.	5:00
IV	TriDent Cloth	1-µm MetaDi Supreme Diamond Suspension	6	150	Comp.	5:00
V	ChemoMet Cloth	MasterPrep 0.05-µm Alumina Suspension	6	150	Contra	2:30
VI	ChemoMet Cloth	MasterMet Colloidal Silica	6	150	Contra	2:30

Table 8: The polishing steps followed for the Hastelloy N and Incoloy 800H samples after corrosion testing. Each sample was mounted in EpoMet, a mineral SiO_2 filled epoxy thermoset, and polished on a Buehler MetaServ®250 with Vector®Power Head. The steps chosen were adapted from the Buehler® *SumMet*™, though each step was repeated or adjusted in response to the polishing progression of the samples [18].

Step	Surface	Abrasive	Load (lbs.)	Base Speed (rpm)	Relative Rotation	Time (min:sec)
I	Carbimet	400 grit SiC	6	150	Contra	Plane
II	UltraPol Cloth	9-µm MetaDi Supreme Diamond Suspension	6	150	Comp.	5:00
III	TriDent Cloth	3-µm MetaDi Supreme Diamond Suspension	6	150	Comp.	5:00
IV	TriDent Cloth	1-µm MetaDi Supreme Diamond Suspension	6	150	Comp.	5:00
V	ChemoMet Cloth	MasterPrep 0.05-µm Alumina Suspension	6	150	Contra	5:00
VI	ChemoMet Cloth	MasterMet Colloidal Silica	6	150	Contra	5:00

Table 9: The polishing steps followed for the Nickel 201 samples after corrosion testing. Each sample was mounted in EpoMet, a mineral SiO_2 filled epoxy thermoset, and polished on a Buehler MetaServ®250 with Vector®Power Head. The steps chosen were adapted from the Buehler® *SumMet*™, though each step was repeated or adjusted in response to the polishing progression of the samples [18].

Step	Surface	Abrasive	Load (lbs.)	Base Speed (rpm)	Relative Rotation	Time (min:sec)
I	Carbimet	400 grit SiC	5	150	Contra	Plane
II	UltraPol Cloth	9-μm MetaDi Supreme Diamond Suspension	6	150	Comp.	5:00
III	TriDent Cloth	3-μm MetaDi Supreme Diamond Suspension	6	150	Comp.	3:00
IV	TriDent Cloth	1-μm MetaDi Supreme Diamond Suspension	6	150	Comp.	2:00
VI	ChemoMet Cloth	MasterMet Colloidal Silica	6	150	Contra	2:00

4 RESULTS AND DISCUSSION

4.1 Alloy Sample SEM Images and Corrosion Rate

Overall, little can be said of the corrosion rate of the samples, given that no sample set showed a clear and consistent linear variation in corrosion depth with test duration. It is possible that the corrosion tests were simply too short in duration to produce results with this linear relationship. However, possible reasons for the lack of a consistent variation in corrosion depth among sample sets, as well as possible sources of error, are further discussed for each alloy.

4.1.1 *Hastelloy N SEM Images and Corrosion Rate*

Upon investigation of the Hastelloy N sample images taken using the JEOL JSM-5910 SEM, shown in Figure 23 on page 36, a corrosion rate cannot be determined via these data alone. The corrosion layer depths of the samples do not appear to vary linearly with the duration of immersion in molten FLiNaK, whether with or without added NiTe. Therefore no corrosion rate has been here determined for Hastelloy N, either by molten FLiNaK with added EuF or by molten FLiNaK with added EuF and NiTe.

Curiously, the corrosion layer of each Hastelloy N sample immersed in FLiNaK salt with added NiTe appears more shallow than the corrosion layer in samples corroded in salt without added NiTe, as evidenced in Figure 23 on page 36. It may be possible that the addition of nickel(II) telluride in conjunction with europium(III) fluoride increases the mitigation effect of the reduction potential. However, this effect, if truly present, would need to be explored in greater depth in future work. The variation in corrosion layer depth may also be due to the fact that oxygen concentrations were unexpectedly elevated during loss of argon cover gas pressure (see Section 3.4.1 on page 26), and the presence of oxygen in the system accelerated corrosion for the samples shown in Figures 23a, 23c, and 23e on page 36.

The sample of Hastelloy N immersed in FLiNaK salt without added NiTe for 100 h shown in Figure 23c on the following page appears at first to contradict this explanation. It was immersed during the third corrosion test (see Section 3.4.4 on page 28) when spikes in oxygen concentration did not occur and the oxygen levels were kept consistently at or below approximately 2 ppm (see Figure 20 on page 31), yet it displays the deepest corrosion layer of any Hastelloy N sample. However, it is important to note that during the third corrosion test when this particular sample was immersed, molten FLiNaK leaked from the nickel crucible and into the glassy carbon containment crucible, possibly giving rise to a galvanic potential that drove corrosion faster in this sample. When taken in conjunction with the unique foam-like corrosion structures apparent in the Nickel 201 sample immersed in FLiNaK with added NiTe for 100 h (see Section 4.1.3 on page 37), the only other sample immersed during the third corrosion test, it remains possible that elevated oxygen concentration is in fact responsible for the greater corrosion layer depths seen in the samples of Hastelloy N immersed in molten FLiNaK without added NiTe for 50 h and 150 h (see Figures 23a and 23e on the following page).

Furthermore, a possible explanation for the indistinct corrosion layer depths amongst a set of Hastelloy N samples immersed for different durations in the same kind of salt may have to do with the adhesive properties of molten FLiNaK. When removing samples from the cooled autoclave, it was noted that hardened salt residue remained on the alloy samples, implying that it had adhered in its molten state to the retracted alloy sample even after that sample's corrosion test duration was complete and the sample had been pulled out of the salt via nickel rod. This continued presence of molten salt on the surface of the alloy sample throughout the duration of the remaining time for the corrosion test would in effect render each sample a 150 h sample, or longer, depending on when cooling was initiated.

4.1.2 Incoloy 800H SEM Images and Corrosion Rate

Similarly to the Hastelloy N samples, but to an even more apparently dramatic extent, the Incoloy 800H samples, shown in Figure 24 on page 38, do not demonstrate any clear, consistent rate of corrosion, either with or without the addition of NiTe to the FLiNaK salt. Possible explanations for this lack of a demonstrable corrosion rate include those discussed for Hastelloy N in Section 4.1.1, including variations in oxygen concentration (see Figures 14 and 17), molten salt adhesion resulting in imprecise corrosion time durations, or any unknown reduction potential effects of added NiTe. None of the Incoloy 800H samples were immersed in salt during the third corrosion test, and therefore it is assumed that none experienced any galvanic corrosion (see Section 3.4.4 on page 28).

However, unlike the Hastelloy N samples, it does not appear that the Incoloy 800H samples immersed in FLiNaK with added NiTe have consistently shallower corrosion layers than those immersed in FLiNaK without added NiTe. In fact, though there is some variability in corrosion along the grain boundaries, the samples immersed in FLiNaK with added NiTe appear to have denser corrosion layers, if not necessarily deeper. For example, in Figure 24f, the corrosion layer appears more uniform in structure along the alloy edge than that of the sample shown in Figure 24e, yet the corrosion could still be said to have reached a similar depth, as it has penetrated into the grain boundary in the sample immersed in FLiNaK without added NiTe for 150 h. This difference in corrosion layer appearance may be accounted

(a) Hastelloy N 50 h in FLiNaK, 1000X

(b) Hastelloy N 50 h in FLiNaK with NiTe, 1000X

(c) Hastelloy N 100 h in FLiNaK, 1000X

(d) Hastelloy N 100 h in FLiNaK with NiTe, 1000X

(e) Hastelloy N 150 h in FLiNaK, 1000X

(f) Hastelloy N 150 h in FLiNaK with NiTe, 1000X

Figure 23: Samples of Hastelloy N after corrosion testing, mounted in EpoMet, polished, coated with gold, and imaged using an SEM. Figures 23a, 23c, and 23e are all Hastelloy N samples that were immersed in Batch I or II salt (see Table 6) without any added NiTe. Figures 23b, 23d, and 23f are all Hastelloy N samples that were immersed in Batch III salt (see Table 6) with added NiTe. All images were taken at a working distance of 10 mm with a spot size of 50 nm and a voltage of 25 kV.

for by Incoloy 800H's large and distinctive grains, which could allow corrosion to occur dramatically along one grain boundary rather than more uniformly along several grain boundaries between smaller grains.

4.1.3 *Nickel 201 SEM Images and Corrosion Rate*

No corrosion rate can be determined using the images taken of the Nickel 201 samples, since no visible corrosion layer could be imaged using the JEOL JSM-5910 SEM. These results are not entirely unexpected, as pure nickel is known to be resistant to corrosion [15].

One notable feature of one Nickel 201 corrosion test sample is a foam-like structure that appears throughout the edge of the sample. In some places, it extends to the edge of the sample while in others, it exists close to the edge, as shown in Figure 25d on page 39. Because this structure does not appear in other Nickel 201 samples tested during this experiment, and because this particular sample was immersed during the third corrosion test (see Section 3.4.4), this structure may be due to an effect arising from the difference in crucibles used for this third test. Although the crucibles for the third corrosion test were made from 99 % nickel foil, they were placed within larger glassy carbon crucibles to contain any potential spills from molten salt leaking from the thin foil crucibles during testing. Given that these foil crucibles leaked into their glassy carbon containers during testing (see Section 3.4.4), a galvanic potential between the nickel and the carbon may have been created, resulting in an additional driver of corrosion that accounts for the structure visible in Figure 25d on page 39.

4.1.4 *316L Stainless Steel SEM Images and Corrosion Rate*

A corrosion rate can not be determined from the imaged samples of 316L Stainless Steel due to the lack of variation in corrosion depth between samples corroded for different time durations, which resulted in no clear linear relationship between corrosion duration and corrosion depth. As discussed for other imaged alloy samples in Sections 4.1.1 and 4.1.2, it is possible that the adhesion of molten FLiNaK to the retracted 50 h and 100 h samples caused each sample to effectively become a 150 h sample, resulting in similar corrosion layer depths for each despite variant immersion time durations.

Similar to the Hastelloy N samples, the corrosion layer for each 316L Stainless Steel sample immersed in FLiNaK containing added NiTe appears more shallow than those of the 316 Stainless Steel samples immersed in FLiNaK without added NiTe, as evidenced in Figure 26 on page 40. Again, it is possible that the addition of NiTe, in conjunction with the added EuF in mixture with the FLiNaK provided some reduction potential effects which slowed the corrosion rate. However, it seems more likely that spikes in oxygen concentration present during the first corrosion test (see Figure 14) account for the greater corrosion layer depth in the 316L Stainless Steel samples immersed in FLiNaK salt without added NiTe.

4.2 Energy-dispersive X-ray Microscopy Scans and Spectra

4.2.1 *Hastelloy N*

An EDS map of the 150 h Hastelloy N sample immersed in FLiNaK salt with added NiTe is displayed in Figure 27 on page 41. As evidenced in Figure 27c, the corrosion of the Hastelloy N did result in apparent chromium

(a) Incoloy 800H 50 h in FLiNaK, 1000X

(b) Incoloy 800H 50 h in FLiNaK with NiTe, 1000X

(c) Incoloy 800H 100 h in FLiNaK, 1000X

(d) Incoloy 800H 100 h in FLiNaK with NiTe, 1000X

(e) Incoloy 800H 150 h in FLiNaK, 1000X

(f) Incoloy 800H 150 h in FLiNaK with NiTe, 1000X
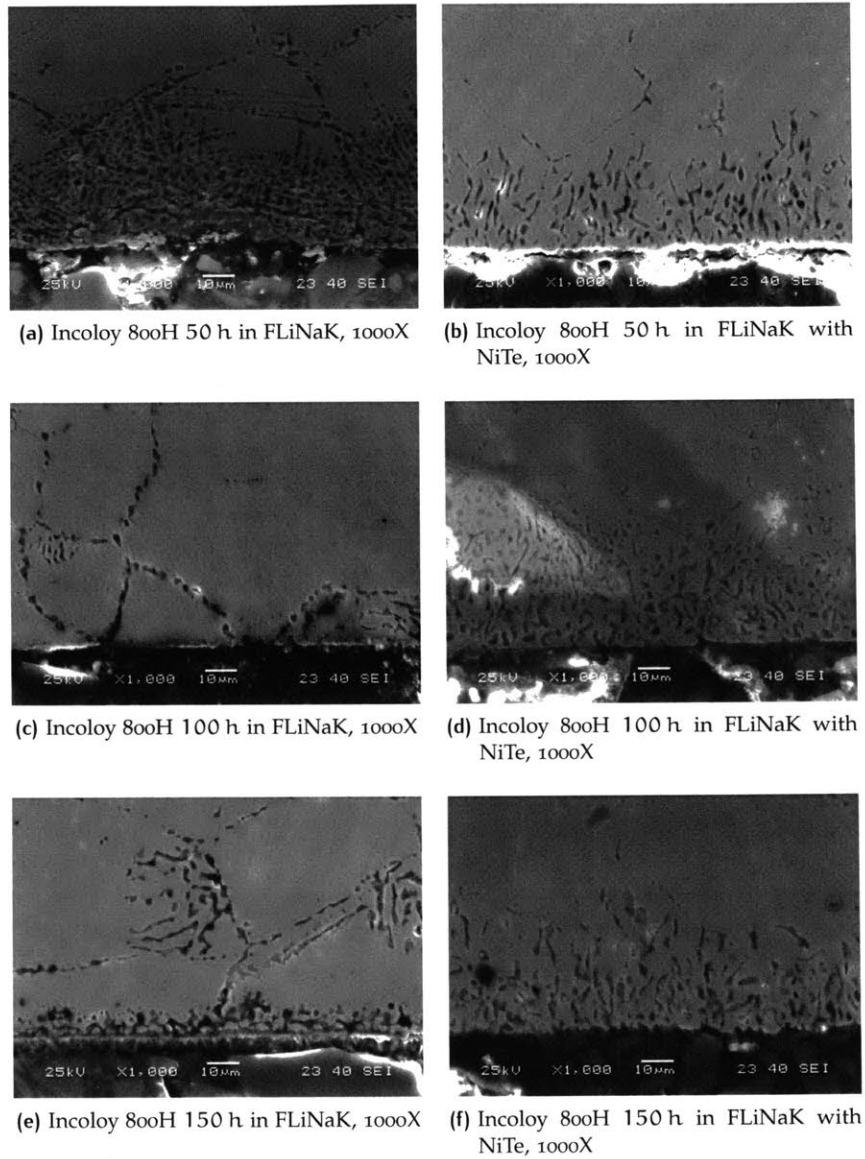
Figure 24: Samples of Incoloy 800H after corrosion testing, mounted in EpoMet, polished, coated with gold, and imaged using an SEM. Figures 24a, 24c, and 24e are all Incoloy 800H samples that were immersed in Batch I or II salt (see Table 6) without any added NiTe. Figures 24b, 24d, and 24f are all Incoloy 800H samples that were immersed in Batch III salt (see Table 6) with added NiTe. All images were taken at a working distance of 23 mm with a spot size of 40 nm and a voltage of 25 kV.

(a) Nickel 201 50 h in FLiNaK, 500X

(b) Nickel 201 50 h in FLiNaK with NiTe, 500X

(c) Nickel 201 100 h in FLiNaK, 500X

(d) Nickel 201 100 h in FLiNaK with NiTe, 500X

(e) Nickel 201 150 h in FLiNaK, 500X
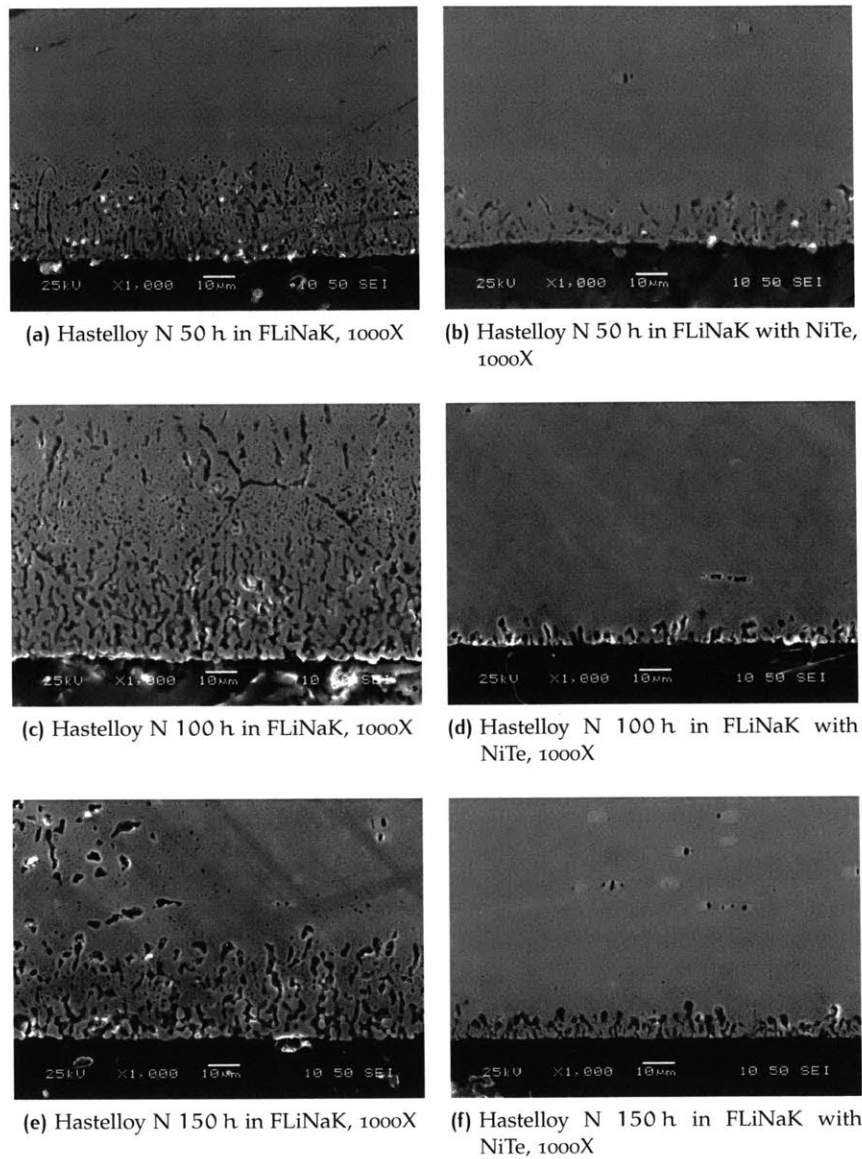
(f) Nickel 201 150 h in FLiNaK with NiTe, 500X
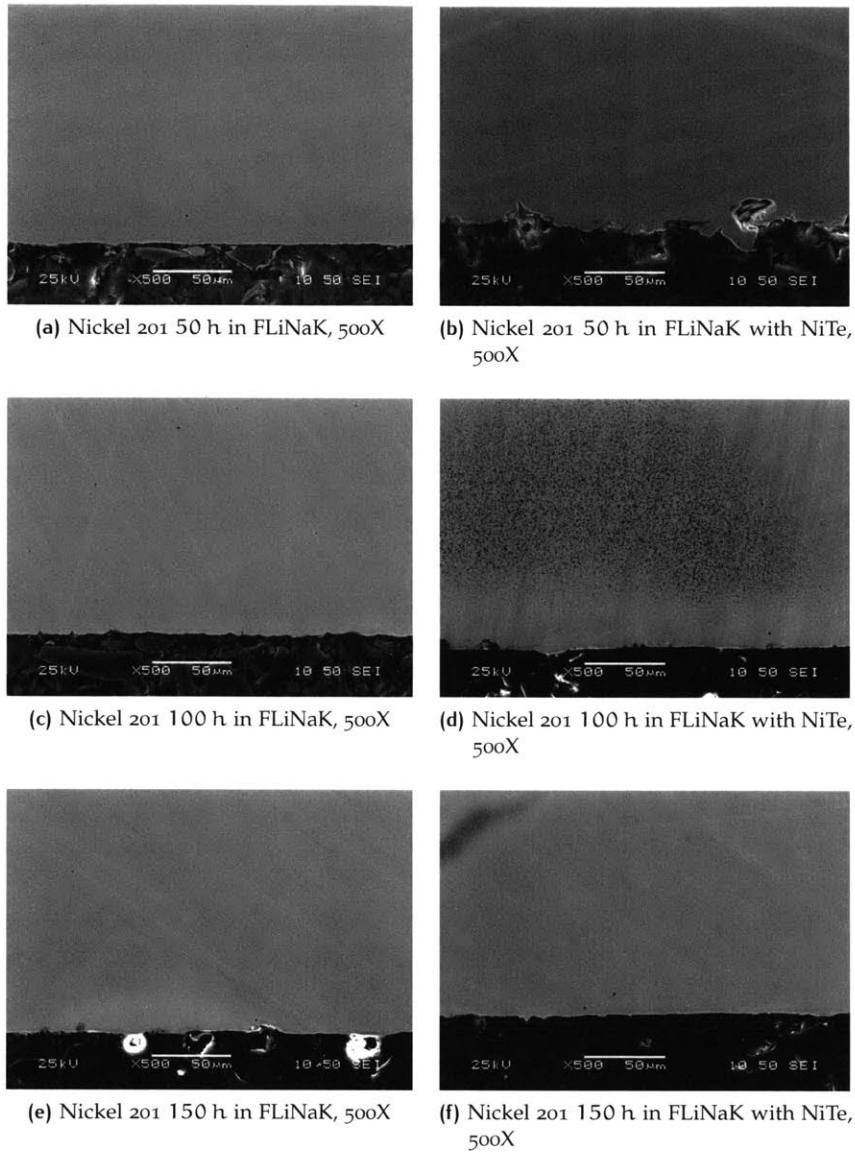
Figure 25: Samples of Nickel 201 after corrosion testing, mounted in EpoMet, polished, coated with gold, and imaged using an SEM. Figures 25a, 25c, and 25e are all Nickel 201 samples that were immersed in Batch I or II salt (see Table 6) without any added NiTe. Figures 25b, 25d, and 25f are all Nickel 201 samples that were immersed in Batch III salt (see Table 6) with added NiTe. All images were taken at a working distance of 10 mm with a spot size of 50 nm and a voltage of 25 kV.
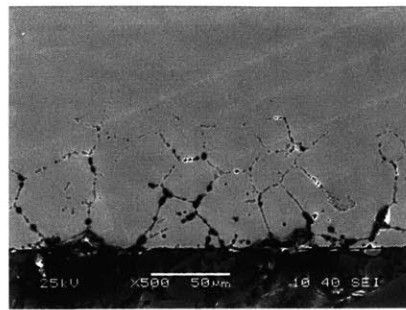
(a) 316L Stainless Steel 50 h in FLiNaK, 500X
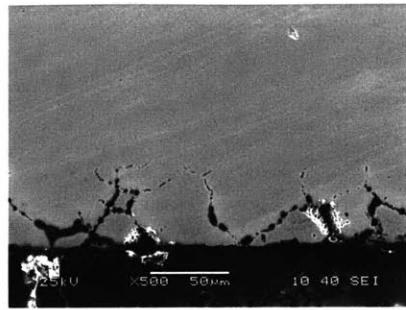
(b) 316L Stainless Steel 50 h in FLiNaK with NiTe, 500X
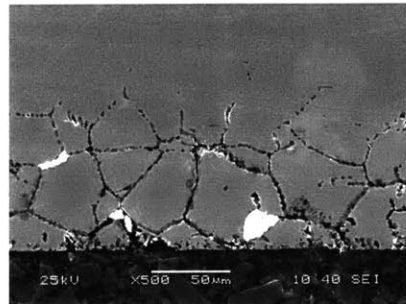
(c) 316L Stainless Steel 100 h in FLiNaK, 500X
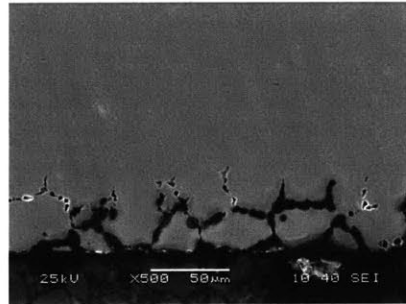
(d) 316L Stainless Steel 100 h in FLiNaK with NiTe, 500X
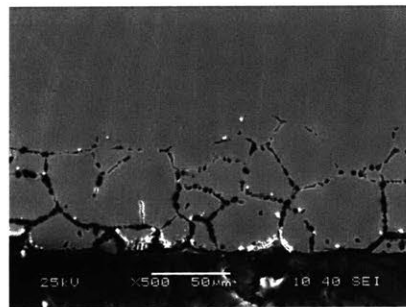
(e) 316L Stainless Steel 150 h in FLiNaK, 500X
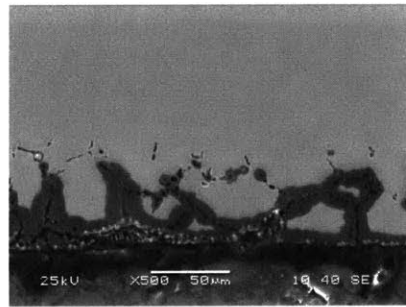
(f) 316L Stainless Steel 150 h in FLiNaK with NiTe, 500X

Figure 26: Samples of 316L Stainless Steel after corrosion testing, mounted in EpoMet, polished, coated with gold, and imaged using an SEM. Figures 26a, 26c, and 26e are all 316L Stainless Steel samples that were immersed in Batch I or II salt (see Table 6) without any added NiTe. Figures 26b, 26d, and 26f are all 316L Stainless Steel samples that were immersed in Batch III salt (see Table 6) with added NiTe. All images were taken at a working distance of 10 mm with a spot size of 40 nm and a voltage of 25 kV.

(a) Iron

(b) Nickel

(c) Chrome

(d) Tellurium
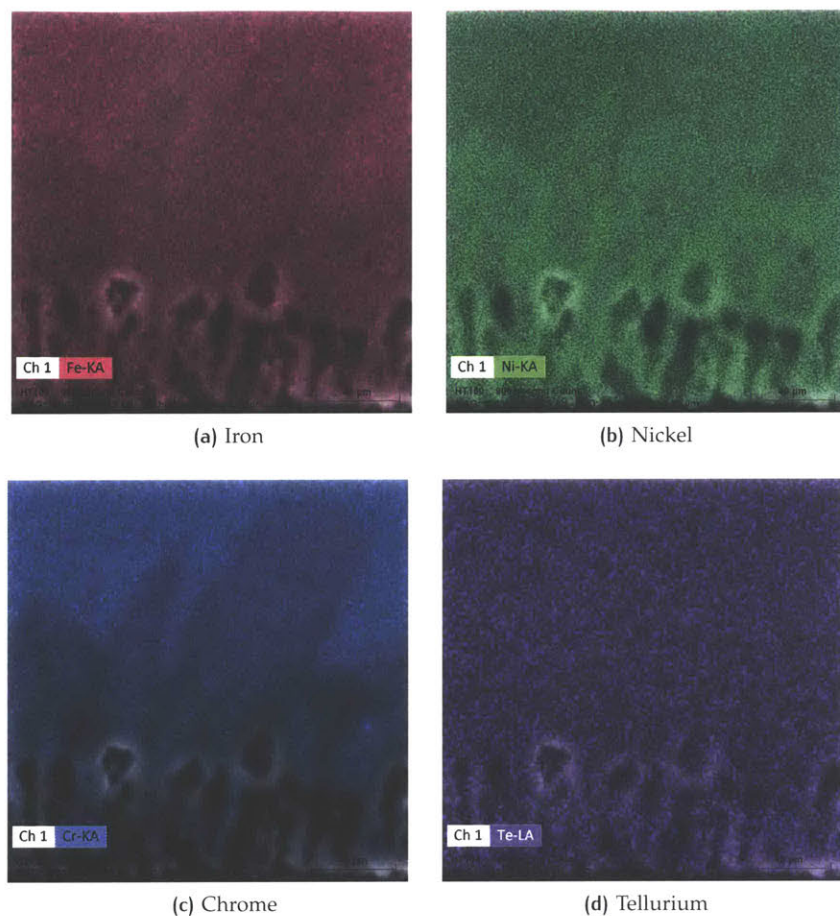
Figure 27: An EDS map of a Hastelloy N sample immersed in FLiNaK salt containing added NiTe at 700 °C for 100 h.

depletion. The iron in Figure 27a appears to have shown some depletion along the corrosion layer as well, though to a lesser extent, whereas the nickel in Figure 27b does not appear to show any such depletion profile. Although Te was an element of key interest for this work, the EDS map in Figure 27d shows no discernible profile for its concentration. This is likely due to the fact that NiTe concentration in the Batch III salt was low at approximately 0.1 wt% (see Table 6 on page 23). Furthermore, the count rate for this particular EDS map was too low to discern areas of high and low concentration, given that little Te was detected at all.

An energy spectrum for this EDS map is given in Figure 28 on the following page. In this spectrum, there is no clear peak at 3.769 kV, the energy of the $L\alpha_1$ x-ray emission line. Furthermore, the count rate was low for this area of the spectrum at under 10 cps, which may account for the lack of a Te peak when the presence of Te was nevertheless anticipated. The prominent peak on the left side of the spectrum is the $K\alpha_1$ spectral emission line for potassium (K). Given potassium's relatively higher concentration in the FLiNaK salt mixture, as well as its close peak proximity to the $L\alpha_1$ peak for Te, the detectability of Te is further obscured.
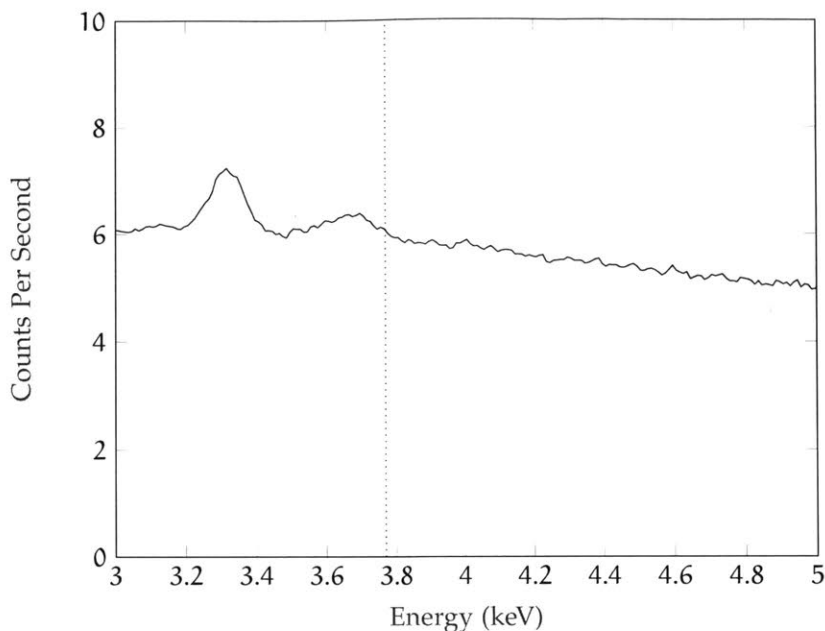
Figure 28: A spectrum resulting from a 900 s count EDS map of Hastelloy N that had been corroded in FLiNaK salt containing added NiTe. Note the lack of a distinct peak at 3.769 kV, the energy of the $L\alpha_1$ emission line for Te.

4.3 Additional Sources of Error and Future Work

In addition to the sources of error already discussed, additional sources of error and limitations to this work should be noted. One such source comes from the location of the thermocouple inserted into the sealed autoclave during corrosion tests. Because it was not long enough to contact either the nickel baseplate or a nickel crucible, the temperature detected by this thermocouple would have been affected by the convection of argon gas moving through the autoclave and could have registered a significantly lower temperature than the molten FLiNaK, which would have been heated through conduction via the nickel baseplate. To achieve a more accurate reading in future work, it may be necessary to adjust the length of the thermocouple such that it touches either the baseplate or the inside of an empty crucible during corrosion tests.

Another source of error arose from difficulties in sample preparation. Specifically, any hardened FLiNaK residue left on sectioned samples after corrosion testing would poorly affect edge retention during mounting in EpoMet and furthermore lead to water condensation and salt crystal growth on polished sample surfaces. It is not known whether and to what extent this salt crystallization and water condensation affected results, but it did have the detrimental effect of making samples more difficult to image. During any future iterations of this work, this effect should be taken into consideration and salt residue must be removed before mounting whenever possible without causing damage to the corrosion layer to be imaged.

In addition, the 1.0 M solution of $Al(NO_3)_3)$ used to clean the crucibles between the first and second corrosion tests (see Section 3.4.2 may have been too strong for its intended purpose, since etching of the Nickel 201 crucibles was observed following their removal from the solution. Though this etching is unlikely to have had any effect on the experiments given

that Nickel 201 is commercially pure, it is possible that some aluminum or nitrate residue was left in the crucible after cleaning. Furthermore, despite polishing attempts with a wire brush, the custom welded base of each nickel crucible left a thin gap in the seam where FLiNaK residue could collect, and this small amount of residue may have affected the results of the second corrosion test. It is recommended that in future work the custom nickel crucibles be modified or replaced with nickel crucibles possessing smooth, polished interiors free from any seams, angles, or roughness in order to facilitate salt removal and cleaning.

Error also arose during EDS analysis of samples. As discussed in Section 4.2.1 on page 37, the count rate was likely too low to observe the $L\alpha_1$ peak for Te. A higher count rate may have been achieved with adjustment of the working distance of the sample in the SEM in order to provide a better angle of x-ray emission toward the detector. Any future study of these or other corrosion test samples should take note and attempt proper adjustments during EDS analysis until a higher count rate can be observed.

Future work should also include longer corrosion durations, so that any differences in corrosion layer depth as it varies with immersion time will become more easily apparent. On a related note, it will be imperative that further iterations of this work resolve the issue of molten FLiNaK adhering to retracted samples during corrosion tests so that each alloy sample will be in contact with molten FLiNaK at 700 °C for only its designated corrosion time. Since it would be difficult to solve the issue of adhesion, it is here recommended that only samples of a given corrosion duration be tested together at one time, and that the furnace be shut off and the system immediately cooled upon retraction of the samples from the molten FLiNaK. Furthermore, to help prevent sample loss during corrosion testing due to wire breakage, it is also recommended that samples be retracted only far enough to remove them from molten salt, but never so far as to hit against the top flange sealing the autoclave.

More possibilities for this research in the future may include altering the composition of the molten salt to include testing in $LiF-UF_4$, a salt that was originally of interest for this work but excluded from testing due to its tendency to oxidize very easily. However, with proper modifications to the experimental setup to reduce oxygen concentration and moisture, and using the knowledge gained from this work, it could be included in corrosion tests in the future. In addition, experimenting with varying concentrations of NiTe in the salt may provide interesting results and help to confirm that while Te can be detected at sufficient concentrations, it is insignificant in low enough quantities. Lastly, more sophisticated equipment and techniques may improve the analysis of future results, such as inductively coupled plasma optical emission spectrometry (ICP-OES) for detection of trace Te and other elements in the salt before and after corrosion tests, or focused ion beam scanning electron microscopy (FIB-SEM) for improved topographical images of the samples.

5   CONCLUSION

Although the results of this work were inconclusive regarding corrosion rate and Te corrosion mechanisms, it nevertheless lays important groundwork for future iterations of these corrosion tests. With the knowledge gained that oxygen concentration appears to make a significant difference in corro-

sion rate, even when due to temporary losses in cover gas pressure, greater care can be taken to keep samples in an oxygen-free atmosphere during corrosion testing by using ultra high purity argon cover gas and avoiding pressure loss. Longer corrosion durations coupled with a solution to the problem of molten FLiNaK adhesion to samples could lead to clear and consistent linear relationships between corrosion depth and immersion duration, giving accurate corrosion rates.

The accidental leakage of molten FLiNaK into glassy carbon crucible containers during a corrosion test that was not originally planned nevertheless yielded the implication that galvanic corrosion would indeed affect these results if the experiments were undertaken with crucibles constructed from materials other than commercially pure nickel, and that care should be taken in future experiments not to introduce any materials that could result in a galvanic couple during corrosion testing. In addition, analytical techniques can be modified and perfected based on the results of this work such that more sensitive detection of Te, as well as higher resolution images of samples, can be gathered and evaluated.

The fact that adding NiTe to molten FLiNaK did not appear to result in greater concentrations of Te in the grain boundaries of any alloys tested is not cause for complacence, as future work may reveal more sophisticated and clearer findings. However, it nevertheless cannot currently be concluded from this work that the addition of NiTe to molten FLiNaK with EuF either accelerates corrosion of Hastelloy N, Incoloy 800H, Nickel 201, or 316L Stainless Steel, or results in telluride compound deposits along the grain boundaries of any of these alloys.

REFERENCES

[1] Hongwei Cheng, Fenfen Han, Yanyan Jia, Zhijun Li, and Xingtai Zhou. Effects of Te on intergranular embrittlement of a Ni-16Mo-7Cr alloy. *Journal of Nuclear Materials*, 2015.

[2] V.V. Ignatiev, A.I. Surenkov, I.P. Gnidoi, V.I. Fedulov, V.S. Uglov, A.V. Panov, V.V. Sagaradze, V.G. Subbotin, A.D. Toropov, V.K. Afonichkin, et al. Investigation of the corrosion resistance of nickel-based alloys in fluoride melts. *Atomic Energy*, 101(4):730–738, 2006.

[3] Victor Ignatiev, Aleksandr Surenkov, Ivan Gnidoi, Vladimir Fedulov, Vadim Uglov, Valery Afonichkin, Andrei Bovet, Vladimir Subbotin, Aleksandr Panov, and Andrei Toropov. Compatibility of selected Ni-based alloys in molten Li, Na, Be/F salts with PuF_3 and tellurium additions. *Nuclear Technology*, 164(1):130–142, 2008.

[4] Victor Ignatiev, Alexander Surenkov, Ivan Gnidoy, Alexander Kulakov, Vadim Uglov, Alexander Vasiliev, and Mikhail Presniakov. Intergranular tellurium cracking of nickel-based alloys in molten Li, Be, Th, U/F salt mixture. *Journal of Nuclear Materials*, 440:243 – 249, 2013.

[5] K. Sridharan and T.R. Allen. Corrosion in molten salts. *Molten Salts Chemistry: From Lab to Applications*, page 241, 2013.

[6] V. Ignatiev and A. Surenkov. Material performance in molten salts. *Comprehensive Nuclear Materials*, 5:221–250, 2012.

[7] Alfred M. Perry. Molten-salt converter reactors. *Annals of Nuclear Energy*, 2(11):809–818, 1975.

[8] Gary S. Was. *Fundamentals of Radiation Materials Science: Metals and Alloys*. Springer Science & Business Media, 2007.

[9] Wenguan Liu, Han Han, Cuilan Ren, Xiujie He, Yanyan Jia, Song Wang, Wei Zhang, Zhijun Li, Xingtai Zhou, Yang Zou, Ping Huai, and Hongjie Xu. First-principles study of intergranular embrittlement induced by Te in the Ni Σ 5 grain boundary. *Computational Materials Science*, 88:22 – 27, 2014.

[10] R.C. Lobb. The effect of tellurium vapour on the creep and tensile properties of 20% Cr-25% Ni–Nb stabilized stainless steel. *Materials Science and Engineering*, 36(2):165–174, 1978.

[11] D.N. Braski and J.M. Leitnaker. Homogenization of Ti-Hastelloy-N. *Metallurgical Transactions A*, 10(4):427–432, 1979.

[12] J.H. DeVan, J.R. DiStefano, W.P. Eatherly, J.R. Keiser, and R.L.. Klueh. Materials considerations for molten salt accelerator-based plutonium conversion systems. Technical report, Oak Ridge National Lab., TN (United States). Funding organisation: USDOE, Washington, DC (United States), 1994.

[13] S. Fabre, C. Cabet, L. Cassayre, P. Chamelot, S. Delepech, J. Finne, L. Massot, and D. Noel. Use of electrochemical techniques to study the corrosion of metals in model fluoride melts. *Journal of Nuclear Materials*, 441:583 – 591, 2013.

[14] Hongwei Cheng, Bin Leng, Kai Chen, Yanyan Jia, Jiasheng Dong, Zhijun Li, and Xingtai Zhou. EPMA and TEM characterization of intergranular tellurium corrosion of Ni–16Mo–7Cr–4Fe superalloy. *Corrosion Science*, 2015.

[15] Corrosion Materials, "Nickel 200/201," CM019-05, Rev. 5. [Online]. Available: http://www.corrosionmaterials.com/documents/ dataSheet/nickel200And201DataSheet.pdf. [Accessed: May 23, 2017].

[16] Corrosion Materials, "Alloy 800H/HT," CM024-07, Rev. 3. [Online]. Available: http://storage.pardot.com/69622/13266/alloy800 DataSheet.pdf. [Accessed: May 23, 2017].

[17] Fine Tubes, "Stainless Steel Alloys 316/316L." [Online]. Available: http://www.finetubes.co.uk/uploads/docs/Fine_Tubes_-_Alloys-316 _316L.pdf. [Accessed: May 23, 2017].

[18] Buehler Ltd. *Buehler® SumMet™: The Science Behind Materials Preparation: A Guide to Materials Preparation & Analysis.* 2007. [Online]. Available: https://shop.buehler.com/sites/default/files/resources/ Buehler_Summet.pdf. [Accessed May 23, 2017].

[19] Shaoqiang Guo, Nikolas Shay, and Jinsuo Zhang. Measurement of europium(III)/europium(II) couple in fluoride molten salt for redox control in a molten salt reactor concept, 2017. Manuscript submitted for publication.

[20] Manohar S. Sohal, Matthias A. Ebner, Piyush Sabharwall, and Phil Sharpe. Engineering database of liquid salt thermophysical and thermochemical properties. *Idaho National Laboratory, Idaho Falls*, 2010.

A   APPENDIX OF DESIGN SPECIFICATIONS

Please see the following pages for design specifications of the autoclave and crucibles that were custom built for the experimental setup.

TOP PLATE, SIDE VIEW

x8 ³/₈"-OD SS TUBES TO WELD TO TOP OF '10" FLANGE

x8 ³/₈"-OD SS TUBES TO WELD TO TOP OF '10" FLANGE

CF FLANGE TO WELD TO TOP OF 10" FLANGE, MDC PART NO. 130008 (PROVIDED)

TOP ↑

10" FLANGE MDC PART NO. 110032

6"

9"

.970"

CUT HOLE THROUGH FOR EACH WELDED TUBE

x6 HOLES TO CUT INTO 10" FLANGE TO MATCH DIAMETER OF HOLES IN WELDED CF FLANGE, THREADING 0.25-28

PROVIDED ASSEMBLY, MDC PART NO. 410003

WELD NEEDED

³/₈"-OD SS TUBE

DRAWING NOT TO SCALE

TOP PLATE, TOP VIEW

* BLUE LINES INDICATE ALIGNMENT WITH
LOWER PLATE

10" FLANGE

×16 ³⁄₈"-OD SS TUBES TO
WELD TO TOP OF 10" FLANGE AND CUT THRU

OUTLINE OF CRUCIBLE ON
BOTTOM PLATE

×5 ¼"-OD
SS TUBE TO
WELD TO TOP
AND CUT THRU
(6" TALL)
24 EXISTING
BOLT HOLES

×6 EXISTING HOLES IN CF FLANGE—
NEED ×6 MATCHING HOLES DRILLED
INTO 10" FLANGE, THREADING .25-28

OUTLINE OF BOTTOM PLATE,
7.5"-OD

CF FLANGE
TO WELD TO
TOP OF PLATE,
2.72"
DIAMETER,
MDC PART NO.
130008
(PROVIDED)

OUTLINE OF HOLE IN BOTTOM
PLATE, 2.875" DIAMETER

RADIUS OF OUTER CIRCLE: 2.98"

RADIUS OF INNER CIRCLE: 2.21"

³⁄₄" DIAMETER HOLE IN CENTER
OF CF FLANGE AND 10" FLANGE,
DRILL THROUGH BOTH
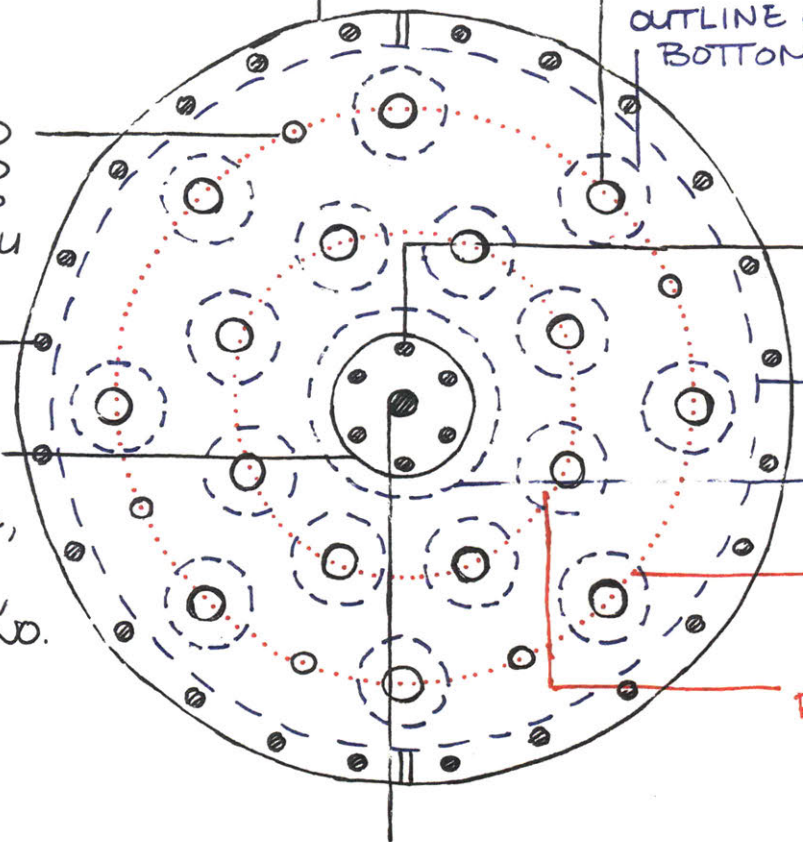
DRAWING, NOT TO SCALE

BOTTOM PLATE, TOP VIEW

7.5" DIAMETER BOTTOM PLATE TO CUT FROM
PROVIDED .25"-THICK Ni-201 PLATE

×1 .25" DIAMETER
HOLE TO CUT AND
THREAD TO MATCH
THREADING ON
ONE Ni-201
ROD

×15 .840" DIAMETER HOLES TO
CUT AND THREAD TO MATCH
THREADING ON CRUCIBLES

RADIUS OF
OUTER
CIRCLE:
2.98"

RADIUS
OF INNER
CIRCLE:
2.21"

×4 .25" DIAMETER Ni-201
RODS TO WELD TO TOP OF
BOTTOM PLATE

2.875" DIAMETER HOLE TO CUT IN PLATE,
CUT THRU
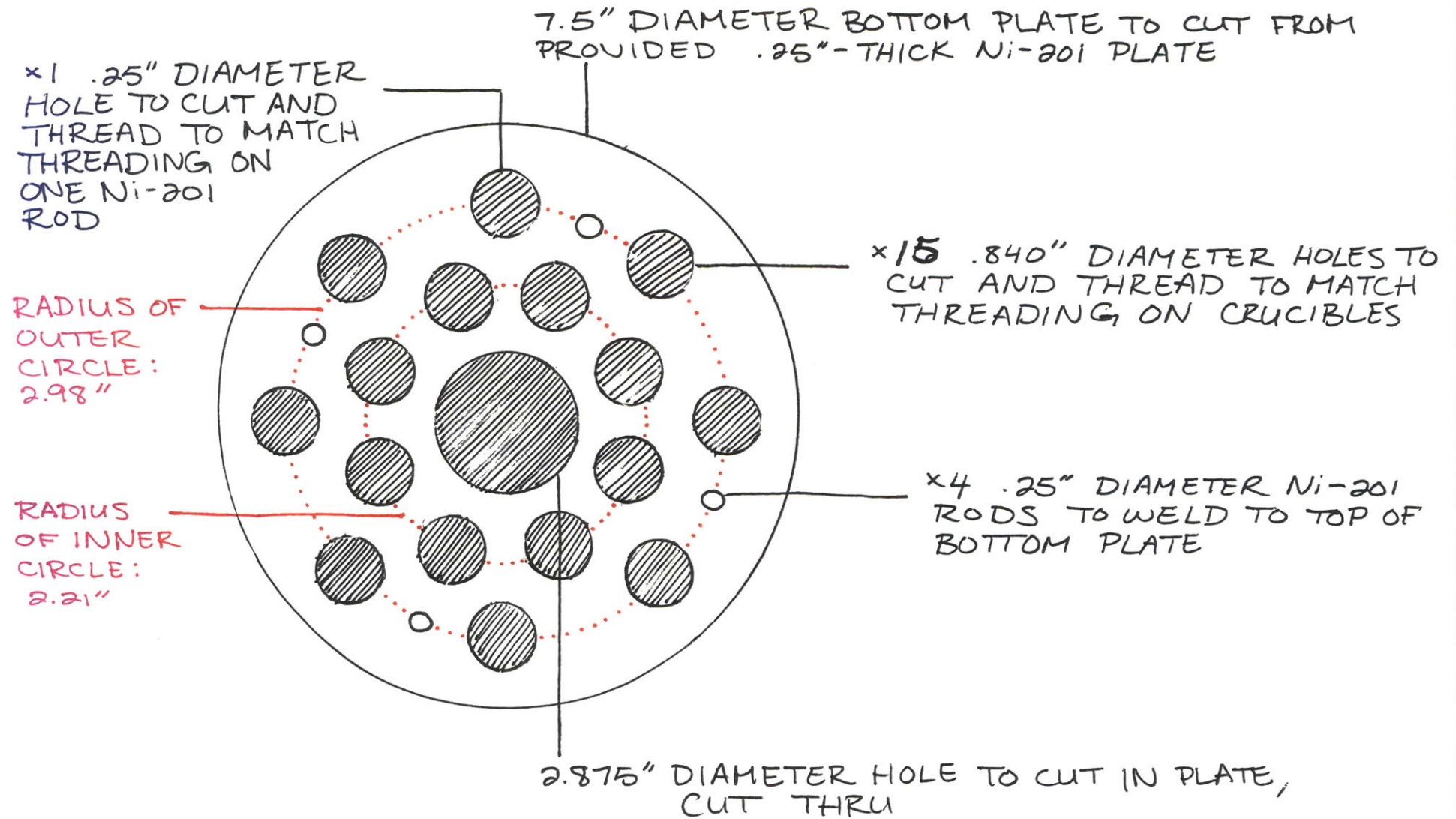
DRAWING NOT TO SCALE

BOTTOM PLATE, SIDE VIEW

Ni - 201

9"

×4 .25" DIAMETER RODS TO WELD TO TOP OF BOTTOM PLATE

7.5" DIAMETER BOTTOM PLATE TO CUT FROM PROVIDED .25"-THICK Ni-201 PLATE

.25"

THREADED HOLES TO HOLD CRUCIBLES

2"

Ni - 201

EXAMPLE OF A SAMPLE CRUCIBLE, THREADED TO MATCH HOLES CUT INTO BOTTOM PLATE, TO CUT FROM PROVIDED Ni-201 TUBING

.840" - OD

.109" THICKNESS

6"

.120" THICKNESS

2.875" - OD
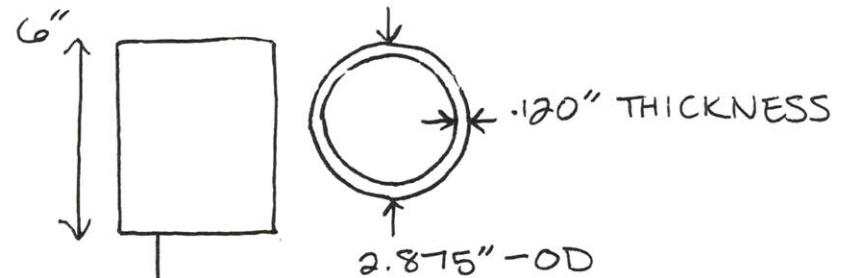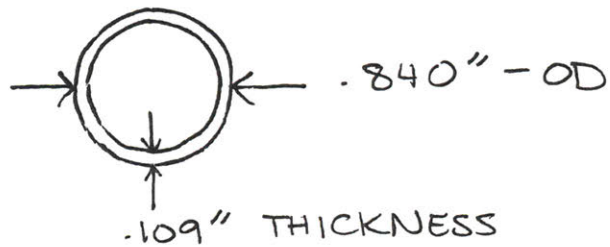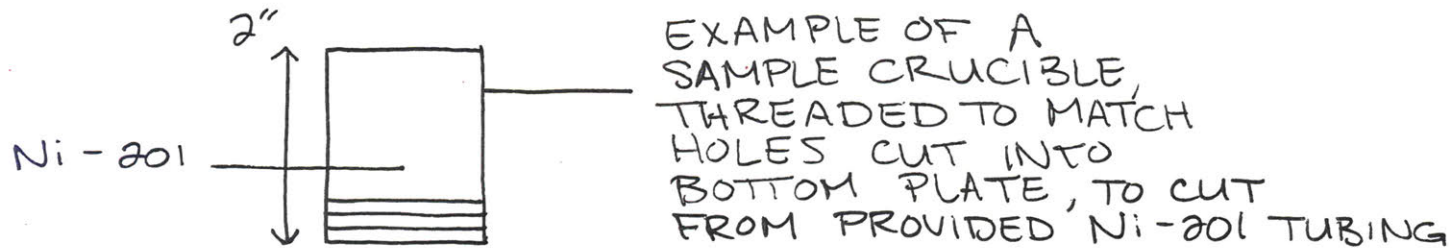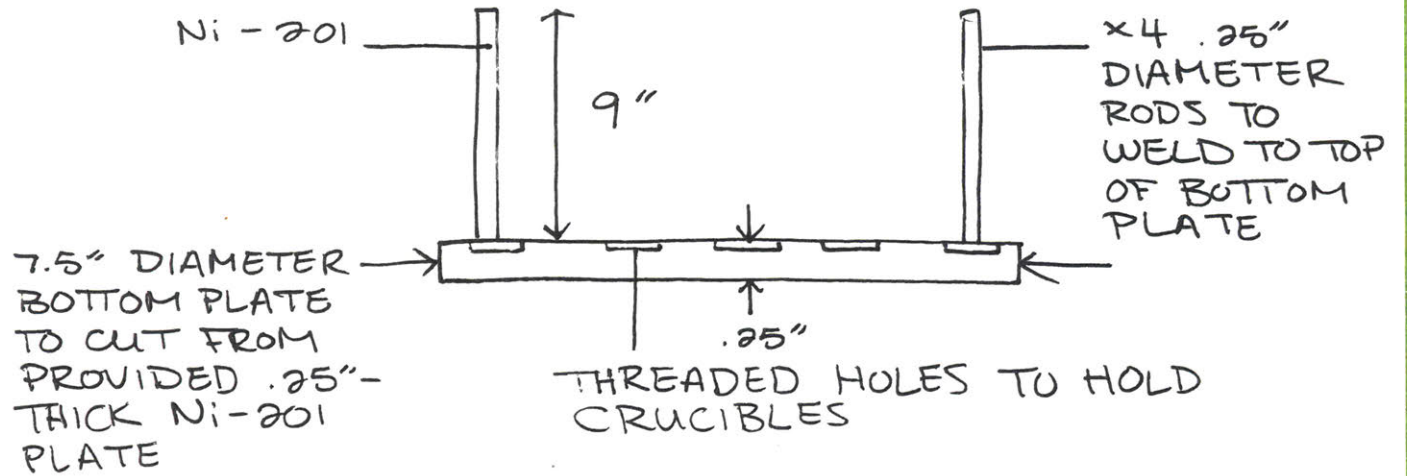
ALSO TO CUT FROM PROVIDED Ni-201 TUBING

DRAWING NOT TO SCALE

B APPENDIX OF CERTIFICATES

B.1 Certificates for Alloy Plate Used for Sample Coupons

Please see the following pages for metallurgical test reports and certificates of analysis for the alloys used for corrosion test sample coupons, Hastelloy N, Nickel 201, Incoloy 800H, and 316L Stainless Steel.

CERTIFICATION OF TESTS • RAPPORT D'ESSAIS CERTIFIE • WERKSZEUGNIS

HAYNES
International

Sales Order No Reference Commande Bestellungs Nr	Date Entered Date De Commande Bestelldatum	Customer Reference Reference Client Kundenbestelldaten	Report No. Rapport Nr Zeugnis Nr	Pages of Pages Page de Pages Anzahl der Seiten
814222-1-0	06/17/2015	21230	20150624113	1 Of 3

Sold To • Client • Bestellanschrift

METAL MEN
PO BOX 54
NEW YORK
NY US

Ship To • Destinataire • Restellmenge

Product Description • Description Produit • Material Beshreibung

0.059 (0.056/0.062) x 36 x 12

HASTELLOY(R) N ALLOY SHEET -

Nadcap Materials Testing Accredited
GE# 19762, S400 2/7/2014, S1000 12/4/2013, EN 10204 3.1, AS9100

Specification • Specification • Spezifikation	Quantity Ordered Quantie Commande Bestellmenge	Quantity Shipped Quantitie Expediee Liefermenge
AMS 5607 E	1 PC	1 PC

Chemical Analysis • Analyse Chimique • Chemische Analyse

Heat Number Numero De Coulee Charge Nr	Al	B	C	Cb+Ta (Nb+Ta)	Co	Cr	Cu	Fe	Mn	Mo	Ni	P	S	Si	Ti	V	W	
2840 1 0011		0.006	0.060		<0.1	6.96	0.06	4.24	0.51	16.91	BAL.	<0.002	<0.002	0.27			<0.1	BUTT END *01

	Ta	Zr	Bi	Se	La		Pb	Mg	Y	Ag	N	Ca	Al+Ti	Ni+Co	Ni+Mo	
2840 1 0011												0.280				BUTT END *01

Certified By • Certifie Par • Bescheinigt Durch: Kristina Brierly
Certification Technician

6/24/2015

(signature)

MIT P.O. 4501928340
1pc) 12" x 24"

(handwritten top right:) Hastelloy-N (C56)

CERTIFICATION OF TESTS • RAPPORT D'ESSAIS CERTIFIE • WERKSZEUGNIS

HAYNES International

Haynes International
1020 West Park Avenue
PO Box 9013
Kokomo, Indiana, 46902

Sales Order No Reference Commande Bestellungs Nr	Date Entered Date De Commande Bestelldatum	Customer Reference Reference Client Kundenbestelldaten	Report No. Rapport No Zeugnis Nr	Pages of Pages Page de Pages Anzahl der Seiten
814222-1-0	06/17/2015	21230	20150624113	2 Of 3

Tensile Test at Room Temperature • Essai De Traction A Temp. Ambiante • Zugversuch Bei Raum Temp.

Ultimate Zugfestigkeit	1% Yield Lim Elast A 1% 1% Streckgrenze	0.2% Yield Lim Elast A 0.2% 0.2% Streckgrenze	% Elong In % Allong EN % Dehnung 2 In	%RA %RA	
113000 PSI		44900 PSI	52 %		1)A)

Tensile Test at Elevated Temperature • Essai De Traction A Hte. Temp. Warm Zugversuch

Test Essai Versuch Temp	Ultimate Zugfestigkeit	1% Yield Lim Elast A 1% 1% Streckgrenze	0.2% Yield Lim Elast A 0.2% 0.2% Streckgrenze	% Elong In % Allong EN % Dehnung	%RA %RA	

Stress Rupture Temperature • Essai A Charge De Rupture Zeitstandversuch

Test Essai Versuch Temp	Stress Constrainte Spannung	Hours Heures Stunden	% Elong In % Allong EN % Dehnung 2 In	% RA	
1500 °F	13000 PSI	166 HRS	32 %		1)A)

Annealed Hardness Durette Recuit Geglueht Haerte	Aged Hardness Durette Vieilli Gealtert Haerte	Grain Size Grosseur De Grain Korngroesse						IGA Attack Depth	Uniformity	Corrosion Rate		Oxidation Rate	Charpy Impact Test				Creep Rupture				
		Grain Size	Predominant Grain Size	Recry Grain	Unrecry Grain %	ALA	P&W Figure Number			Corrosion MPY	Test Method		Toughness Avg Ft Lbs	Toughness 1 Ft Lbs	Toughness 2 Ft Lbs	Toughness 3 Ft Lbs	Test Essai Versuch Temp	Stress Constrainte Spannung PSI	Hours Heures Stunden	% Elong In % Allong EN % Dehnung	% Elong In 15 Hrs
86 HRBW	1)A)	4.5						0.0001 IN													

Certified By • Certifie Par • Bescheinigt Durch: **Kristina Brierly**
Certification Technician

6/24/2015   1) 3465245701

[signature: Brierly]

Sales Order No eference Commande Bestellungs Nr	Date Entered Date De Commande Bestelldatum	Customer Reference Reference Client Kundenbestelldaten	Report No. Rapport No. Zeugnis Nr	Pages of Pages Page de Pages Anzahl der Seiten
814222-1-0	06/17/2015	21230	20150624113	3 Of 3

CERTIFICATION OF TESTS • RAPPORT D'ESSAIS CERTIFIE • WERKSZEUGNIS

HAYNES International

Haynes International
1020 West Park Avenue
PO Box 9013
Kokomo, Indiana, 46902

ll tests and inspections have been performed and results meet specification requirements.
HIS MATERIAL IS FREE FROM MERCURY, CADMIUM, RADIUM, AND ALPHA SOURCE CONTAMINATION.
HIS MATERIAL WAS MELTED AND MANUFACTURED IN THE UNITED STATES.
Vhen microstructure analysis is performed, the etchant used is H2O2 and HCl. Samples were viewed at 100-500x magnification. Grain size evaluation is performed to the requirements of ASTM E112-96(2004)e2 Plate 1. Samples
re prepared per ASTM E3-01. The material has been evaluated for alloy depletion
his material conforms to all technical requirements of AMS 5607.
his material has been annealed and cooled in a protective atmosphere.
his material has passed the bend test as specified in AMS 5607.
Aill Orders Used: 3465245701 (1 PC)
l) 2125 °F to 2175 °F
Aethod of Chemistry Analysis for Heat# 10011 BUTT END *01: ARL-3460 DIRECT RATIO (B.P): LECO (C.S): XARL LINFIT (ALTI,Co,Cr,Cu,Fe,Mn,Mo,Ni,Si,W).

Certified By • Certifie Par • Bescheinigt Durch: Kristina Brierly   6/24/2015
Certification Technician

✱ATI Allegheny Ludlum | Certificate of Test

Stephen Wolff - Director, Corporate Quality Assurance

	Mill Information	Customer Information

**500 Green Street
Washington, PA 15301**

Cert Number	0128406-00	
Sales Order	50-034-048	
Cert Date	Apr-23-2014	PO Date Mar-04-2014

| Sold to: | METALMEN SALES, INC.
P.O. BOX 14
NEW YORK NY 10044 | Ship to: | MIT P.O. 4501924197
2 pcs) 12" x 12" |
|---|---|---|---|

Material Information

"ATI 200/201" NICKEL
PMP HOT ROLLED PLATE ANNEALED PICKLED COMMERCIAL CUT EDGE

ASME-SB-162 ED 2013	ASTM-B-162-99 R2009
UNS N02200	UNS N02201

Piece Information

Pcs	Gauge (in)	Width (in)	Length (in)	Heat #	Piece ID	Section Id	Lot #	Total Wt (lbs)
Item: 002	Cust-Id:
Cust-Job:			Govt-Contract-#:
ScheduleB:			Govt-DO-Rating:	
1	.2500	96.0000	258.0000	07L4A78-02	AB46520	---	433938	2047
1	.2500	96.0000	288.0000	07L4A78-01	AB46537	---	433938	2285
1	.2500	96.0000	288.0000	07L4A78-01	AB46539	---	433938	2285

Chemistry Testing

Element	Requirements Min	Requirements Max	Final Heat Analysis 07L4A78-01	Loc	Final Heat Analysis 07L4A78-02	Loc
C	---	.02	.01	TC	.01	TC
MN	---	.35	< .01	BN	< .01	BN
S	---	.010	< .001	TC	< .001	TC
SI	---	.35	.05	BN	.06	BN
NI	99.00	---	BAL	--	BAL	--
CU	---	.25	< .01	BN	< .01	BN
TI	---	---	.001	BN	.001	BN
FE	---	.40	.01	BN	.01	BN
MG	---	---	.008	BN	.008	BN

Allegheny Ludlum performs chemical analysis by the following techniques:
C, S by combustion/infrared; N, O, H by inert fusion/thermal conductivity;
Mn, P, Si, Cr, Ni, Mo, Cu, Cb, Co, V, by WDXRF; Pb, Bi, Ag by GFAA;
B by OES; Al and Ti (>=0.10%) by WDXRF, otherwise by OES.

✳ATI Allegheny Ludlum | Certificate of Test

Stephen Wolff - Director, Corporate Quality Assuranc

	Mill Information	Customer Information
500 Green Street Washington, PA 15301	Cert Number 0128406-00 Sales Order 50-034-048 Cert Date Apr-23-2014	PO Date Mar-04-2014

Chemistry Testing

07L4A7801	- Material was produced by VIM and ESR.
07L4A7802	- Material was produced by VIM and ESR.

Mechanical Testing

		LOT 433938	
Condition:		ANNEALED	
Direction:		TRANSVERSE	
Temperature:		ROOM TEMP	
Spec:			
Test Limit	**Units**	**Result**	**Loc**
YIELD 0.2%	psi	29100.	TC
TENSILE	psi	55500.	TC
ELONGATION	%	52.	TC
RED OF AREA	%	87.	TC
HARDNESS	---	100. HBW	TC

When hardness is measured using the Brinell scale, the indentation measuring device is Type A.

Mechanical Property Requirements

Condition:		ANNEALED	
Direction:		TRANSVERSE	
Temperature:		ROOM TEMP	
Spec:			
Test Limit	**Units**	**Min**	**Max**
YIELD 0.2%	psi	15000.	---
TENSILE	psi	55000.	---
ELONGATION	%	40.	---
RED OF AREA	%	---	---
HARDNESS	---	---	---

Metallography - General

Test ID	Result Name	Condition	Test Result	Loc	Requirements
LOT 433938	GRAIN SIZE	ANNEALED	5.	TC	---

Metallographic magnification: 100X;   Etchant used HCL/NITRIC/ACETIC MIXED ACID

ALC720   04/23/2014 13:07:19

✴ATI Allegheny Ludlum | Certificate of Test

Stephen Wolff - Director, Corporate Quality Assurance

	Mill Information		Customer Information
500 Green Street **Washington, PA 15301**	Cert Number	0128406-00	
	Sales Order	50-034-048	
	Cert Date	Apr-23-2014	PO Date Mar-04-2014

Certification Statements

Material was solution annealed at 1350F (732C) minimum for a time commensurate with thickness.

Allegheny Ludlum does not use mercury in the testing or production of its products.

Material is of USA melt and manufacture.

No welds/weld repairs performed.

Knowingly and willfully recording any false, fictitious or fraudulent statement or entry on this document may be punished as a felony under Federal Statutes, including Federal Law, Title 18, Chapter 47.

DIN EN 10204:2005 3.1 Certificate

General Statements

TESTING WAS PERFORMED AT THE FOLLOWING LOCATIONS
   BN = ATI-ALLEGHENY LUDLUM; 100 River Road; Brackenridge, PA 15014
   TC = ATI-ALLEGHENY LUDLUM; 1300 Pacific Avenue; Natrona Heights, PA 15065
WARNING: Processing that makes fumes, dust, or solutions may cause lung disease. Please see MSDS for further information which has been supplied to your Purchasing Department. For an additional copy, please refer to our web site at
www.atimetals.com/businesses/business-units/ludlum/Pages/msds.aspx.

For access to online Certifications of Test, please register at www.alcextra.com.

The above is a true copy of the data on file. The material and test results conform to the sales contract and specification(s) as set forth in ATI Allegheny Ludlum's order acknowledgement. This certificate of Test may not be reproduced except in full without the written authorization of the company.

ATI Allegheny Ludlum's website contains a listing of material produced, general technical and contact information, and current quality and company accreditations including but not limited to ISO-9001, AS-9100, Nadcap, and ISO/IEC 17025. Please visit us at www.atimetals.com

Incoley 800H Plate (handwritten)

GREAT LAKES

metalmen sales inc
po box 54
NY, NY 10044

HUNTINGTON ALLOYS
A Special Metals Company
HUNTINGTON, WEST VIRGINIA 25720

CERTIFIED MATERIAL TEST REPORT No. 58312

HA ORDER NO./ITEM	DATE	PAGE	OF
300007622 1	10/29/02	1	1

QUANTITY	INSPECTED BY
3367 LBS	HA/SMC

CHARGE ORDER NO.	MARK ORDER NO.
578328-21344310	578320-21344310

DESCRIPTION OF MATERIAL SHIPPED: INCOLOY ALLOY 800H/800HT   CR SHEET PKL ANN
.1250 IN   48.0000 IN COIL   COIL

THIS IS TO CERTIFY THAT ALL REQUIRED SAMPLINGS INSPECTIONS AND TESTS HAVE BEEN PERFORMED IN ACCORDANCE WITH THE ORDER AND SPECIFICATION REQUIREMENTS. THE TEST REPORT REPRESENTS THE ACTUAL ATTRIBUTES OF THE MATERIAL FURNISHED AND THE VALUES SHOWN ARE CORRECT AND THE MATERIAL DESCRIBED BY THIS CERTIFICATE IS IN FULL COMPLIANCE WITH ALL ORDER AND INSPECTION REQUIREMENTS. WE HEREBY CERTIFY THAT IF BELOW FILLERS ARE IN ACCORDANCE WITH THE SPECIFIED CONTRACT REQUIREMENTS.

QUALITY CERTIFICATION REPRESENTATIVE

********THIS REPORT RELATES ONLY TO THE ITEM(S) TESTED AND MAY NOT BE REPRODUCED EXCEPT IN FULL.********

SPECIFICATIONS: HAI 328 REV F\ASTM B 409-01 SIZE PER ORDER\
ASME SB-409 2001 EDITION NO ADDENDA SIZE PER ORDER.\
QUALITY SYSTEM CERTIFICATION: ISO 9002 (ABS-QE CERT. 30125);
EN 10 204/DIN 50049 (CERT.3.1.B)

UNS:N08810/N08811

CHEMICAL ANALYSIS (WT. %)

HEAT#	C	MN	FE	S	SI	CU	NI	CR	AL
	TI	AL+TI							
HH6276AG	0.08	0.76	45.78	<0.001	0.27	0.39	31.84	19.94	0.46
	0.48	0.94							

MELT METHOD: EF/AOD + ELECTROSLAG REMELTED

MECHANICAL PROPERTIES

HEAT/LOT	QUANTITY	HARDNESS	GRAIN SIZE	YIELD .2%PSI X 100	TENSILE PSI X 100	%ELG 2"	R/A %	DEG F
HH6276AG CX04H	1 PC							
ROOM TEMP-HRB -AS SHIPPED		72.3		0349	0851	45.9		

GRAIN SIZE-AS SHIPPED AGS ASTM NO.   3.5
NORMAL - TRAN
YIELD STRENGTH WAS DETERMINED USING A STRESS STRAIN CURVE

VISUAL AND DIMENSIONAL EXAMINATION SATISFACTORY.
MATERIAL, WHEN SHIPPED, IS FREE FROM CONTAMINATION BY MERCURY, RADIUM, ALPHA SOURCE, & LOW MELTING ELEMENTS.
AUTHORIZED QUALITY CERTIFICATION REPRESENTATIVES:
W.E. BOLEN, P.D. CUSTER, A.L. MILLS, M.A. MORRISON, D.L. SMITH, P.P. WAUGH

MIT P.O. 4501961710 (handwritten)
(pc) 15¾" x 20" (handwritten)

316L SS Plate

METALLURGICAL TEST REPORT

NAS
289 Mifflin Drive

Pennsylvania
289 Mifflin Drive
Wrightsville, PA 17368
USA

Certificate: 3562 1   Mail To: Ship To:

Date: 11/07/2014   Page: 1

Customer: 002275 013   METALMEN SALES, INC.
P.O. BOX 54
NEW YORK NY 10044

Steel: 316/316L

Finish: 1

Your Order: P41105WJ001   NAS Order: IN 0201339 01

Corrosion: ASTM A262/02aE;180Bend-OK

PRODUCT DESCRIPTION:
STAINLESS STEEL COIL, HRAP; UNS 31600/31603
ASTM A240/13c,A480/13,A666/10;ASME SA240/13,SA480/13,SA666/13
CHEM ONLY ON FOLLOWING ASTM: A276/13,A479/13a,A484/13a,A312/13
CHEM ONLY ON FOLLOWING ASME: SA312/11,SA479/11
AMS 5507G/5524L X MRK;
NACE MR0175/ISO 15156-3:2003 A , MR0103/07; QQS766D-A X MAG PERM
MIN. SOLUTION ANNEAL TEMP 1900F, WATER QUENCHED
SAE AMS QQ-S-763

REMARKS:
Mat'l is Free of Mercury Contamination. No weld repairs.
EN 10204:2004 3.1; RoHS 1 & 2 Compliant
Material is Free of Radioactive Contamination
NAS Steel Making Process: EAF, AOD, & Cont. Casting
Product Mfg.by a Quality Mgt.Sys. in Conf. w/ISO 9001
*Melted & Manufactured in the USA; Mat'l is DFARs Compliant

Product Id	Coil #	Skid #	Thickness	Width	Weight	-------Length------	Mark	Pieces	Commodity Code
01R1F7 A	01R1F7 A		.2440	48.0000	13,600	COIL		1	1

CHEMICAL ANALYSIS   CM(Country of Melt) ES(Spain) US(United States) ZA(South Africa) JP(Japan)

Chemical Analysis per ASTM A751/08

HEAT	CM	C %	CR %	CU %	MN %	MO %	N %	NI %	P %	S %
R1F7	US	.0256	16.7135	.4545	1.2395	2.0315	.0552	10.0350	.0295	.0010

		SI %								
		.3290								

MECHANICAL PROPERTIES

Product Id#	Coil #	l o c	d i r	UTS KSI	20C .2% YS 20C KSI	ELONG %-2"	% Hard RB	Tail Hard
01R1F7 A	01R1F7 A	F	T	87.15	45.72	50.84	84.00	89.00

*MIT P.O. 4501924197
2pcs) 12" x 12"*

NAS hereby certifies that the analysis on this certification is correct. Based upon the results and the accuracy of the test methods used, the material meets the specifications stated. These results relate only to the items tested and this report cannot be reproduced, except in its entirety, without the written approval of NAS.

Technical Dept. Mgr.

ABHIJEET BHAVE   11/07/2014

B.2   Certificates for Alloys Used for Experiment Construction

Please see the following pages for metallurgical test reports and certificates of analysis for the materials used in constructing the experimental setup for this work.

SALZGITTER
MANNESMANN
STAINLESS TUBES

Salzgitter Mannesmann Stainless Tubes USA, Inc   (A01)

12050 West Little York - Houston, TX 77041 - USA

www.smst-tubes.com

INSPECTION CERTIFICATE
Abnahmeprüfzeugnis
Certificat de réception

EN 10204 2004 TYPE 3.1   (A02)

Page/Seite
1/3

No/Nr/N (A03)

246799-5

METALMEN SALES, INC.
P.O. BOX 54
NEW YORK NY 10044

Purchaser/Besteller/Acheteur

Customer order no./Kunde Auftragsnr./N° Commande client (A07)

112320

SMST-Tubes order no/Auftragsnr./N° Commande (A08)

0000246799

SMST-Tubes item   Part number/Teilenummer/N° d'article (A09)

0000246799-000005

Product Description/Produkt Beschreibung/Description du produit (B01) (B02) (B04)

Seamless Nickel Alloy Cold Finished Pipes in Bright Condition Plain Ends Square Cut Deburred
Kaltgefertigte nahtlose Edelstahlrohre in Bright Condition Enden Glatt Abgeschnitten
Pipes en Acier Inox Sans Soudure Finis à Froid in Bright Condition Coupes d'equerre, lisses, ébavure

Specifications/Spezifikationen/Spécifications   ASME SB 161 11 a >US units / ASTM B 161 05 >US units

Grade/Werkstoff/Nuance   UNS N02200 / UNS N02201

Tolerances/Toleranzen/Tolérances   ASTM B 829

Marking of the product/Kennzeichnung des Produktes/Marquage du produit(B06-D01)
DMV NPS 1/2" X SCH 40 UNS-N02200/UNS-N02201 B/SB-161 HT 115058 SML CF 246799-5 HYDRO PHU(XXX) QL50002639 USA

Quantity/Menge/Quantité						Dimensions		Abmessungen		
Heat no Schmelze Nr N° de Coulée	Quality lot Qualitätslos Lot qualité	SMST item	Pieces Stück Pieces (B08)	Total weight Gesamtgewicht Masse totale (B13)	Total length Gesamtlänge Longueur totale	OD (B09)	WT (B10)	Tube length Rohrlänge Longueur tube		
								min	(B11)	max
115058	QL50002639	000005	62	1275 Lbs	1 274.41 Ft	0.840 "	0.109 "	17 Ft		24 Ft

Chemical Analysis / Chemische Zusammensetzung / Analyse chimique (C71 - C92)

Heat no/Schmelzen Nr./N° de coulée   115058

Melting Process/Erschmelzungsart/Élaboration (C70)   E+AOD or VOD

Heat Origin/Ursp. der Schmelze/Origine de la Coule   Germany

Heat Analysis / Analyse de coulée

	C	Si	Mn	S	Ni	Cu
Min	0.00	0.00	0.00	0.0000	99.0	0.00
Max	0.020	0.35	0.35	0.0100	99.99	0.25
	0.013	0.05	0.15	<0.002	99.60	<0.01

	Fe
	0.00
Max	0.40
	0.05

MIT P.O. 4501924197
2pcs) 5 ft Long

SALZGITTER MANNESMANN STAINLESS TUBES

Salzgitter Mannesmann Stainless Tubes USA, Inc   (A01)

12050 West Little York - Houston, TX 77041 - USA

www.smst-tubes.com

INSPECTION CERTIFICATE
Abnahmeprüfzeugnis
Certificat de réception

No/Nr/N°   (A03)

246799-5

EN 10204. 2004 TYPE 3.1   (A02)

Mechanical testing

Quality Lot : QL50002639

Tensile test at room temperature/Zugversuch bei Raumtemperatur/Essai de traction à température ambiante (C10)

ASTM E 8

Test no Proben Nr. N° d'échantillon (C00)	Direction Probenricht ung Direction (C02)	Yield strength/Dehngrenze/Limite d'elasticité (C11)			Tensile strength / Zugfestigkeit / Résistance à la traction (C12)	Elongation/Bruchdehnung/Allongement (C13)					Reduction of area Z%
		0.2 %	0.5 %	1 %		2 "	50 mm	5D	5,65 √So	4D	
		psi	/	/	psi	%	/	/	/	/	/
	Min	15000	/	!	55000	35	/	/	/	/	/
	Max	/	/	/	/	!	/	/	/	/	.
50010550	LONGITUDINAL	17099 95	/	/	59401 66	46 00	/	!	/	/	:

Hardness test/Härteprüfung/Essai de dureté (C30)

ASTM A 370

Test no Proben Nr. N° d'echantill on	HB			HRC			Load / HV			HRB			HR 15-T			HR 30-T		
Min	/	/	/	:	/	/	!	/	/	:	/	/	/	/	/	/	/	:
Max	/	/	/	/	:	/	/	i	/	/	/	:	:	/	:	/	!	/
	min	max	avg	min	max	avg	min	max	avg	min	max	avg	min	max	avg	min	max	avg
50010550	/	/	:	:	:	/	/	/	/	/	/	/	78.0	80.0	79 00	J	i	:

Salzgitter Mannesmann Stainless Tubes USA, Inc

SALZGITTER
MANNESMANN
STAINLESS TUBES

Salzgitter Mannesmann Stainless Tubes USA, Inc   (A01)

12050 West Little York - Houston, TX 77041 - USA

www.smst-tubes.com

Page/Seite

3/3

No/Nr/N° (A03)

246799-5

INSPECTION CERTIFICATE
Abnahmeprüfzeugnis
Certificat de réception

EN 10204 2004 TYPE 3.1   (A02)

Other Tests and Declarations / Andere Prüfungen und Prüffeststellungen / Autres tests et déclarations

QL50002639

Heat Treatment in protective atmosphere rapid gas cooling. 1450°F and Air Cooled

Hydrostatic tested / 1,000 PSi / 5 Seond hold

No Weld repair / Keine Reparaturschweissung / Aucune réparation par soudure

The material is conforming to directive 2000/53/EC, 2002/95/EC and CD 2005/618/EC. / Das Material entspricht den Anforderungen der Richtlinien 2000/53/EC, 2002/95/EC und CD 2005/618/EC. / Le matériau est conforme aux directives 2000/53/EC, 2002/95/EC et CD 2005/618/EC

Tubes are free from mercury contamination and from radioactive contamination / Die Rohre sind frei von Quecksilberverunreinigungen und frei vom radioaktiver Verunreinigung / Les tubes sont exempts de contamination par le mercure et de contamination radioactive

Confirmation with reference to Pressure Equipment Directive 97/23/EC
The works operates a quality management system that has undergone a specific assessment for materials for pressure equipment and is certified by a competent body (ABS QE Cert. No. 30788)
Bestätigung in Bezug auf Druckgeräterichtlinie 97/23/EC
Das Werk wendet ein Qualitätsmanagementsystem an, das in Bezug auf Werkstoffe für Druckgeräte einer spezifischen Bewertung unterzogen wurde und von einer zuständigen Stelle (ABS QE Cert. No. 30788) zertifiziert ist.
Confirmation concernant la Directive Equipements sous Pression 97/23/EC L'usine applique un système de management de la qualité qui a fait l'objet d'une évaluation spécifique pour les matériaux pour équipements sous pression et qui est certifié par un organisme compétent (ABS QE Cert. No 30788)

BRIGHT ANNEALED @ 3.20 FPM @ 1450°F AND AIR COOLED

Material When Shipped Is Free From Contamination by Mercury. Radium, Alpha Source and Low Melting Elements.

SMST certify that the delivered products comply with the requirements stipulated in the order. / Die Erzeugnisse wurden bestellungsgemäß geprüft und für in Ordnung befunden. / SMST-Tubes atteste que les produits livrés sont conformes aux stipulations de la commande

Validation by manufacturer's representative / Validierung durch Vertreter des Herstellers

Mill's Inspector
Werksachverständiger
Le contrôleur usine

Raynee Rangel - Quality Technical Analyst

Date of edition
Ausgabedatum   18/09/2012
Date d'édition

Ni-201
¼" Bar

AM Alliant Metals, Inc.
134B - Route 111 - Hampstead, NH 03841
Tel (603) 329-4488 • Fax (603) 329-4317

Order #: **260476**

Print Info: 10/21/15 - 12:09:37 - JEAN

| Customer #: 777
 MIT
 PO BOX 9169
 Cambridge, MA 021392343
 (617) 253-6070 | \<Ship To\>
 MIT
 32 VASSAR ST
 Cambridge, MA 02139
 (617) 253-1000 | \<Notes\>
 ***IF PURCHASE ORDER GIVEN THEY ARE ON TERMS
 OTHERVISE USE CREDIT CARD ******
 PLEASE FAX INVOICES TO APPROPRIATE CUSTOMERS
 ---ship 72" lengths approx unless noted otherwise |

F.O.B.: DESTINATION

Cust PO: **Richard Belanger**

Entered By: DEVIN

Ship Via: UPS Ground-Commercial (Zone 1)

Pay Terms: Credit Card-no disc avail

UPS ($): 302.95

Order Date: 10/16/15

Ship Date: 10/22/15

LI	QTY ORD.	DESCRIPTION	ITEM CD COLOR	QTY SHIP	Heat#
		MISC MATERIAL ITEM- X 72.00"			
1	3 EA	3 piece of Nick 201 1/4" dia x 72"	31298 No Color	3 EA @ 72" 3 LB	NN68U3AR15

RECEIVED OCT 2 2 2015 BY:

R. Belanger (3)

BOX:	SKID:	PC:	BDL:	TB:
0	0	0	0	0

Customer Signature:

Customer Copy

HUNTINGTON ALLOYS CORPORATION
3200 Riverside Drive, Huntington, West Virginia 25705-1771 USA
Tel: +1.304.526.5100   Toll-Free in the USA: 1.800.334.4626
Fax: +1.304.526.5643   Info@specialmetals.com

SPECIAL METALS
A PCC Company

Certificate No. 28794-00

Dated		02-JAN-14

CERTIFIED MATERIALS TEST REPORT

Page No.   1 / 3

Note: The recording of false, fictitious or
fraudulent statements or entries on this
document may be punishable as a felony
under federal statute.

This report relates only to the item(s) tested
and may not be reproduced except in full.

Sales Order Number	Purchase Order Number	Mark Order Number	Material Heat / Lot Identity
100058700 / 1.1	037612-3	037612-3	NN68U3AR15

UNS Number

N02200/N02201

Material Description

NICKEL 200/201, AIR INDUCTION MELTED,   , HOT ROLLED ROD - COIL, PICKLED, ANNEALED, .3120, IN
5 PCS   4956 LBS

Specifications

ASTM B160-05 (2009) CHEM ONLY / ASME SB-160 2010 EDITION 11 ADDENDA CHEM ONLY / A-1 NI200/201
MOD FOR CUST. 1269 & 721 REV 3-23-09.

ANALYSIS

	C %	MN %	FE %	S %	SI %	CO %	NI %	TI %	MG %
	.01	.23	.011	.001	.08	.023	99.2	.05	.02
Method	C/S	XR26	XR26	C/S	XR26	XR26	XR26	XR26	OES

	CO %	MO %	AS %	SB %	V %
	.001	.00146	<.000001	<.000001	.00005
Method	OES	XR26	ICP-MS	ICP-MS	XR26

	NI+CO
	99.2
Method	

ANALYSIS METHOD LEGEND

RECEIVED

OCT 2 2 2015

BY: ....

SPECIAL METALS
A PCC Company

HUNTINGTON ALLOYS CORPORATION
3200 Riverside Drive, Huntington, West Virginia 25705-1771 USA
Tel: +1.304.526.5100   Toll-Free in the USA: 1.800.334.4626
Fax: +1.304.526.5643   info@specialmetals.com

Certificate No. 28794-00

Dated   02-JAN-14

CERTIFIED MATERIALS TEST REPORT

Page No.   2 / 3

XRF - X-Ray Fluorescence
ICP - Inductively Coupled Plasma
C/S - Carbon/Sulfur
OES - Optical Emission Spectoscopy
XRF6 - X-Ray Fluorescence 2600

TENSILE TEST

ROOM TEMP TENSILE - LONG | LAB | MECHANICAL

PIECE ID	TEST TEMPER	HARDNESS	HARD TYPE	TENSILE KSI	.2% YIELD KSI	EFF GA LNGTH IN	RED OF AREA	ELONG
1	AN	21.2	HRB	55.2	13.5	2.000	89.3	61.4

ORIENT

LONG

OTHER TESTS

GRAIN SIZE MEASUREMENT | LAB | METALLOGRAPHY

PIECE ID	TEST TEMPER	TEST ORIENT	AV GS ASTM	NRM or DUP
1	AN	TRANSVERSE	3.5	NORMAL

NO WELDING OR WELD REPAIR WAS PERFORMED.
LOCATION LEGEND: B = BACK   C = CENTER   F = FRONT   H = HEAD   M = MIDDLE   T = TOE

COUNTRY OF ORIGIN: MELTED AND MANUFACTURED IN THE USA
THIS CERTIFICATION AFFIRMS THAT THE CONTENTS OF THIS REPORT ARE CORRECT AND ACCURATE AND THAT ALL TEST RESULTS AND
OPERATIONS PERFORMED BY SPECIAL METALS CORPORATION, INC. OR ITS SUBCONTRACTORS ARE IN COMPLIANCE WITH THE MATERIAL
SPECIFICATIONS AND THE SPECIFIC APPLICABLE MATERIAL REQUIREMENTS OF ASME SECTION III.
ASME QUALITY SYSTEMS CERTIFICATE QSC-328, EXPIRES 3/25/2014.
AS APPLICABLE ANY SUBCONTRACTED WORK ALSO COMPLIES WITH CUSTOMER AND ASME SECTION III, NCA 3800 REQUIREMENTS.
QUALITY SYSTEM MEETS REQUIREMENTS OF DIRECTIVE 97-23/EC (PRESSURE EQUIPMENT DIRECTIVE),
ANNEX 1, CHAPTER 4.3 PER ABS GROUP LTD CERTIFICATE 41734 (EXPIRES JULY 30, 2014)."

HUNTINGTON ALLOYS CORPORATION IS AN ACCREDITED INDEPENDENT NADCAP MATERIALS TESTING LABORATORY VIA CERTI-
FICATE NUMBER 127895 (EXPIRES OCTOBER 31, 2014) FOR ALL TESTING SPECIFIED IN THE SCOPE OF ACCREDITATION.
MATERIAL PRODUCED UNDER QA SYSTEM DOCUMENTED IN HUNTINGTON ALLOYS CORP QA MANUAL REV. 30, DATED 4/8/2013
QUALITY SYSTEM CERTIFICATION: ISO 9001:2008 (ABS-QE CERT. 30125); EN 10 204/DIN 50049 (TYPE 3.1)

RECEIVED
OCT 2 2 2015

BY: ....

HUNTINGTON ALLOYS CORPORATION
3200 Riverside Drive, Huntington, West Virginia 25705-1771 USA
Tel: +1.304.526.5100   Toll-Free in the USA: 1.800.334.4626
Fax: +1.304.526.5643   info@specialmetals.com

Certificate No. 28794-00

Dated   02-JAN-14

CERTIFIED MATERIALS TEST REPORT   Page No.   3 / 3

LABORATORY IS ACCREDITED TO ISO/IEC 17025:2005 FOR MECHANICAL TESTING AND CHEMICAL ANALYSIS.

VISUAL AND DIMENSIONAL EXAMINATION SATISFACTORY.
MATERIAL, WHEN SHIPPED, IS FREE FROM CONTAMINATION BY MERCURY, RADIUM, ALPHA SOURCE, AND LOW MELTING ELEMENTS.

CHEMICAL ANALYSIS AS REQUIRED FOR CARBON, SULFUR, NITROGEN, OR OXYGEN IS PERFORMED BY COMBUSTION TECHNIQUES.
ALL OTHER REPORTED ELEMENTS ARE ANALYZED BY X-RAY AND/OR EMISSION SPECTROSCOPY. ""

AUTHORIZED QUALITY CERTIFICATION REPRESENTATIVES:
W. B. NOLEN, D. K. MILLER, K. R. SMITH, G. J. BURKHEAD

CERTIFIED TESTING LABORATORY DATA SOURCE IATI AEBG VENDOR NO. 47150 N. R. E. CASE RECORD NO. : NONE

AUTHORIZED VENDOR SIGNATURE   DK M.Q.   DATE 1-3-14

End Of Certificate

This is to certify that all required samplings inspections and tests have been performed in accordance with the order and specification requirements. The test report represents the actual attributes of the material furnished and the values shown are correct and true. The material described by this certificate is in full compliance with all order and inspection requirements. We hereby certify that the figures given are in accordance with the specified contract requirements.   REV. 8/08

Signed

DK M.Q.

For and on behalf of HUNTINGTON ALLOYS CORPORATION
Authorized Signature

BRIGHTRAY, CORRONEL, FERRY, INCOCLAD, INCOLOY, INCONEL, INCOTHERM, INCO-WELD, KOTHERM, MAXORB, MONEL, NILO, NILOMAG, NIMONIC, NIOTHERM, NI-SPAN, UDIMET & WIGGIN are trademarks of the Special Metals group of companies

RECEIVED

OCT 2 2 2015

BY: ....

CERTIFICATE OF TEST

ALLIANT SPECIALTY METALS
134B RT 111
HAMPSTEAD, NH 03841

DATE: 10/19/15

CONTROL NUMBER: 155517
SPECIFICATION:
    ASTM B 160

ATTENTION: DEVIN FORD

P.O. #: 112581

GRADE: NICKEL 201
             COLD DRAWN
             ANNEALED

HEAT #: 015140521

DESC: ROD
CONDITION: CENTERLESS GROUND

CHEMICAL ANALYSIS			
NI:	99.2	MG:	.02
MN:	.23	FE:	.011
SI:	.08	C:	.01
TI:	.05	CO:	.001
CU:	.023	S:	.001

MECHANICAL PROPERTIES

ELONGATION: 59%

YIELD STRENGTH: 45,000 PSI

TENSILE STRENGTH: 58,000 PSI

Comments: MILL HEAT: NN68U3AR15

SIZE: .250 x 72.000in

Material meets DFARS Clause 252.225-7008 / 7009.
Melted in the U.S. or qualifying country in accordance
with 225.003(10) or by interpretation of the definition
of SPECIALTY METALS as referenced in the clause.

Raw materials which are used at National Electronic Alloys
are NOT mined or processed in the DEMOCRATIC REPUBLIC
OF THE CONGO (DRC) or an ADJOINING COUNTRY and
are in conformance with Section 1502 of the Dodd-Frank
Wall Street Reform and Consumer Protection Act of 2010.

SIGNED: _____
          (QUALITY CONTROL)

RECEIVED
OCT 2 2 2015

BY: ....

1

CERTIFIED MILL TEST REPORT

DMV STAINLESS USA, INC.
12020 W Little York • Houston, TX 77041
Phone 713-466-7278 • Fax 713-466-3769

Customer:

DMV Order Number: 222273-2A

METALMEN SALES, INC.
P.O. BOX 14
NEW YORK, NY 10044

Material: 2-1/2" SCH 10 DMV-200/201 (UNS NO2200/UNS NO2201)

Specification(s): COLD FINISHED SEAMLESS NICKEL ALLOY PIPE PER ASTM-B161-03,ASME-SB-161-04.PRODUCTION IN COMPLIANCE WITH CERTIFICATE 3.1.B ACC. TO EN 10204-8-91 AMEND. A1-8-95.MATERIAL SHIPPED FREE FROM CONTAMINATION BY MERCURY,RADIUM,ALPHA SOURCES AND LOW MELTING ELEMENTS.SOLUTION BRIGHT ANNEALED AND PASSIVATED.

Material Marking: DMV 2 1/2" SCH 10 TP UNS-NO2200/UNS-NO2201 B/SB-161 HT M00905 SMLS COLD FIN 222273-2A HYDRO-TESTED MADE IN USA

Pcs No	Weight	Total Length	OD		WT		Min Length 17'-0" Ft	Max Length 24'-0" Ft
18	Lbs	416'-3" Ft	2-1/2"	NPS	SCH	10		

Heat No: M00905

	C	Mn	P	S	Si	Ni	Cr	Mo	N	Cu	Ti	Al	B	V	Co	Fe	CB + TA
Min						99.00				0.25						0.40	
Max	0.02	0.35		0.010	0.35	99.50				0.00						0.08	
Ladle	0.012	0.270		0.001	0.046												
Product																	
Product																	

Mechanical and Metallurgical Properties:

LONG:	Requirements:	Yield - Min 15 KSI	Tensile - Min 55 KSI	Elongation - Min 35%
	Results:	15.1	57.1	46%

FLATTENING:	Samples:	Result:
HARDNESS: HR	Samples:	Result:
MICROSTRUCTURE:	Samples:	Result:
FLARE:	Samples:	Result:

Additional testing / comments:

Visual and dimensional examination with satisfactory results.

NDT: Hydrostatic Test   1000   PSI   5 Second Hold   ACC.

Heat Treatment: 1450 ° F   Solution annealed and cooled to less than 800 ° F within 2 minutes

PMI examination: OK

We certify that the material herein described has been manufactured, inspected and tested in accordance with and satisfies the requirements of the above referenced specifications. This material has not been repaired by welding and has not been in contact with Mercury nor its compounds. Marking materials contain less than 250 ppm each sulphur and total halogens which may be detrimental to the materials upon heating.

Jim Bates - Lab Supervisor *Jim Bates*

MIT P.O. 4501924197
(pc) 12"L

Heat # M00905
Code 210SN2-5
Vendor DMV
PO # 65951

VERIFIED

December 7, 2006

Page 1 of 1

8468

Material Certification Report

Ni-201 ¼" Bar *(handwritten)*

Certification ID:5641

METALMEN
Produced On: 01/12/15
Reference: GFM

Sales Order: 87195-01
Part #:
Purchase Order #: *MIT P.O. 4501924197* *(handwritten)*

2pcs) S Fr L *(handwritten)*

MATERIAL DESCRIPTION
Heat #: NN68U9AR14
Alloy: 200/201
UNS: N02200/201

Lot #: G3444
Size: 0.25"DIA
Form: Bar

Specifications: COLD WORKED (AS WORKED); UNS N02200: ASTM B160-05 (2014); UNS N02201: ASTM B160-05 (2014) (CHEM ONLY)

CHEMICAL ANALYSIS (% WT)
C: .01   Co: .001   Cu: .015   Fe: .011   Mg: .01   Mo: .00022   Mn: .28
Ni: 99.3   S: .002   Si: .11   Ti: .1   V: .00007
As & Sb: <.000001

TENSILE PROPERTIES AT ROOM TEMPERATURE
Result 1:
Ultimate (psi): 89,700
0.2% Yield (psi): 82,800
Elongation: 25.0%   4D
Reduction of Area: 80.9%
Hardness: 88 HRBW

COMMENTS
MELTED AND MANUFACTURED IN USA

STATEMENTS
We certify that the material shipped to you have been tested in accordance with and conforms to the listed specification(s). The recording of false, fictitious, or fraudulent statements on this document may be punishable as a felony under Federal Statutes, including Federal Law Title 18, Chapter 47.
This material was melted and manufactured in compliance with DFARS 252.225-7014 ALT. 1.
No welding or weld repair was performed on this material.
This material was produced without known contact with: Mercury or its components, Lead or its components, or other materials containing low melting point metals as a basic chemical constituent.

David L. Morrow *(signature)*

David L. Morrow, QA Manager   06/09/15

Material Certification Report

Ni - 201
¼" Bar

Certification ID: 5641

METALMEN

Produced On: 01/12/15
Reference: GFM

Sales Order: 87195-01
Part #:
Purchase Order #: *MIT P.O. 4501968892*
5pcs) 6 Ft L

MATERIAL DESCRIPTION

Heat #: NN68U9AR14
Alloy: 200/201
UNS: N02200/201

Lot #: G3444
Size: 0.25"DIA
Form: Bar

Specifications: COLD WORKED (AS WORKED); UNS N02200: ASTM B160-05 (2014); UNS N02201: ASTM B160-05 (2014) (CHEM ONLY)

CHEMICAL ANALYSIS (% WT)

C: .01   Co: .001   Cu: .015   Fe: .011   Mg: .01   Mo: .00022   Mn: .28
Ni: 99.3   S: .002   Si: .11   Ti: .1   V: .00007
As & Sb: <.000001

TENSILE PROPERTIES AT ROOM TEMPERATURE

Result 1:
Ultimate (psi): 89,700
0.2% Yield (psi): 82,800
Elongation: 25.0%   4D
Reduction of Area: 80.9%
Hardness: 88 HRBW

COMMENTS

MELTED AND MANUFACTURED IN USA

STATEMENTS

We certify that the material shipped to you have been tested in accordance with and conforms to the listed specification(s).
The recording of false, fictitious, or fraudulent statements on this document may be punishable as a felony under Federal Statutes, including Federal Law Title 18, Chapter 47.
This material was melted and manufactured in compliance with DFARS 252 225-7014 ALT. 1.
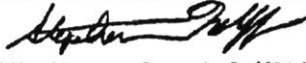No welding or weld repair was performed on this material.
This material was produced without known contact with: Mercury or its components, Lead or its components, or other materials containing low melting point metals as a basic chemical constituent.

David L. Morrow
David L. Morrow, QA Manager   06/09/15

�֍ATI Allegheny Ludlum | Certificate of Test

Stephen Wolff - Director, Corporate Quality Assurance

	Mill Information	Customer Information
500 Green Street Washington, PA 15301	Cert Number 0128406-00 Sales Order 50-034-048 Cert Date Apr-23-2014	PO Date Mar-04-2014

Sold to:	~~METALMEN SALES, INC.~~ ~~P.O. BOX 14~~ ~~NEW YORK, NY 10044~~	Ship to:	MIT P.O. 4501924197 2 pcs) 12" x 12"

Material Information

"ATI 200/201" NICKEL
PMP HOT ROLLED PLATE ANNEALED PICKLED COMMERCIAL CUT EDGE

ASME-SB-162 ED 2013	ASTM-B-162-99 R2009
UNS N02200	UNS N02201

Piece Information

Pcs	Gauge (in)	Width (in)	Length (in)	Heat #	Piece ID	Section Id	Lot #	Total Wt (lbs)
Item: 002	Cust-Id: Cust-Job:			Govt-Contract-#: ScheduleB:			Govt-DO-Rating:	
1	.2500	96.0000	258.0000	07L4A78-02	AB46520	---	433938	2047
1	.2500	96.0000	288.0000	07L4A78-01	AB46537	---	433938	2285
1	.2500	96.0000	288.0000	07L4A78-01	AB46539	---	433938	2285

Chemistry Testing

Element	Requirements Min	Requirements Max	Final Heat Analysis 07L4A78-01	Loc	Final Heat Analysis 07L4A78-02	Loc
C	---	.02	.01	TC	.01	TC
MN	---	.35	< .01	BN	< .01	BN
S	---	.010	< .001	TC	< .001	TC
SI	---	.35	.05	BN	.06	BN
NI	99.00	---	BAL	--	BAL	--
CU	---	.25	< .01	BN	< .01	BN
TI	---	---	.001	BN	.001	BN
FE	---	.40	.01	BN	.01	BN
MG	---	---	.008	BN	.008	BN

Allegheny Ludlum performs chemical analysis by the following techniques:
C, S by combustion/infrared; N, O, H by inert fusion/thermal conductivity;
Mn, P, Si, Cr, Ni, Mo, Cu, Cb, Co, V, by WDXRF; Pb, Bi, Ag by GFAA;
B by OES; Al and Ti (>=0.10%) by WDXRF, otherwise by OES.

✹ATI Allegheny Ludlum | Certificate of Test

Stephen Wolff

Stephen Wolff - Director, Corporate Quality Assurance

	Mill Information		Customer Information
500 Green Street Washington, PA 15301	Cert Number	0128406-00	
	Sales Order	50-034-048	
	Cert Date	Apr-23-2014	PO Date Mar-04-2014

Chemistry Testing

```
07L4A7801  - Material was produced by VIM and ESR.
07L4A7802  - Material was produced by VIM and ESR.
```

Mechanical Testing

		LOT 433938	
Condition:		ANNEALED	
Direction:		TRANSVERSE	
Temperature:		ROOM TEMP	
Spec:			
Test Limit	Units	Result	Loc
YIELD 0.2%	psi	29100.	TC
TENSILE	psi	55500.	TC
ELONGATION	%	52.	TC
RED OF AREA	%	87.	TC
HARDNESS	---	100. HBW	TC

When hardness is measured using the Brinell scale, the indentation measuring device is Type A.

Mechanical Property Requirements

Condition:		ANNEALED	
Direction:		TRANSVERSE	
Temperature:		ROOM TEMP	
Spec:			
Test Limit	Units	Min	Max
YIELD 0.2%	psi	15000.	---
TENSILE	psi	55000.	---
ELONGATION	%	40.	---
RED OF AREA	%	---	---
HARDNESS	---	---	---

Metallography - General

Test ID	Result Name	Condition	Test Result	Loc	Requirements
LOT 433938	GRAIN SIZE	ANNEALED	5.	TC	---

Metallographic magnification: 100X;   Etchant used HCL/NITRIC/ACETIC MIXED ACID

ALC720 04/23/2014 13:07:39

✳ATI Allegheny Ludlum	**Certificate of Test**	*Stephen Wolff*	
		Stephen Wolff - Director, Corporate Quality Assuranc	
	Mill Information	**Customer Information**	
500 Green Street Washington, PA 15301	Cert Number 0128406-00		
	Sales Order 50-034-048		
	Cert Date Apr-23-2014	PO Date Mar-04-2014	

Certification Statements

Material was solution annealed at 1350F (732C) minimum for a time commensurate with thickness.

Allegheny Ludlum does not use mercury in the testing or production of its products.

Material is of USA melt and manufacture.

No welds/weld repairs performed.

Knowingly and willfully recording any false, fictitious or fraudulent statement or entry on this document may be punished as a felony under Federal Statutes, including Federal Law, Title 18, Chapter 47.

DIN EN 10204:2005 3.1 Certificate

General Statements

TESTING WAS PERFORMED AT THE FOLLOWING LOCATIONS
    BN = ATI-ALLEGHENY LUDLUM; 100 River Road; Brackenridge, PA 15014
    TC = ATI-ALLEGHENY LUDLUM; 1300 Pacific Avenue; Natrona Heights, PA 15065
WARNING: Processing that makes fumes, dust, or solutions may cause lung disease. Please see MSDS for further information which has been supplied to your Purchasing Department. For an additional copy, please refer to our web site at
www.atimetals.com/businesses/business-units/ludlum/Pages/msds.aspx.

For access to online Certifications of Test, please register at www.alcextra.com.

The above is a true copy of the data on file. The material and test results conform to the sales contract and specification(s) as set forth in ATI Allegheny Ludlum's order acknowledgement. This certificate of Test may not be reproduced except in full without the written authorization of the company.

ATI Allegheny Ludlum's website contains a listing of material produced, general technical and contact information, and current quality and company accreditations including but not limited to ISO-9001, AS-9100, Nadcap, and ISO/IEC 17025. Please visit us at www.atimetals.com

C   APPENDIX OF DATA

Please see supplemental files for raw data collected on oxygen, temperature, and moisture of the argon cover gas used during corrosion tests.